AIR FORCE INSTITUTE OF TECHNOLOGY

AIR UNIVERSITY
UNITED STATES AIR FORCE

APPLICATION OF THE HYDRAULIC SYSTEM
FREQUENCY RESPONSE PROGRAM TO
PROPELLANT FEED SYSTEMS
THESIS

AFIT/GA/AA/80M-1   BRYAN S. DEHOFF
CAPT, USAF

SCHOOL OF ENGINEERING

DTIC
ELECTE
MAR 2 9 1985
B

WRIGHT-PATTERSON AIR FORCE BASE, OHIO

85   03   13   063

AFIT/GA/AA/80M-1

APP_ICATION OF THE HYDRAULIC SYSTEM
FREQUENCY RESPONSE PROGRAM TO
PROPELLANT FEED SYSTEMS
THESIS

AFIT/GA/AA/80M-1   BRYAN S. DEHOFF
CAPT, USAF

DTIC
ELECTE
MAR 2 9 1985

B

AFIT/GA/AA/80M-1

APPLICATION OF THE HYDRAULIC SYSTEM
FREQUENCY RESPONSE PROGRAM TO
PROPELLANT FEED SYSTEMS

THESIS

Presented to the Faculty of the School of Engineering
of the Air Force Institute of Technology
Air University
in partial fullment of the
requirements for the Degree of Master of Science

by
Bryan S. DeHoff, B.S.M.E.M.
Capt, USAF
Graduate Astronautical Engineering
December 1984

Preface

I wish to thank all those who have encouraged me during this lengthy study. Special thanks go to my advisor, Dr Milton E. Franke for his guidance; my supervisors in the Solid Rocket Division, Air Force Rocket Propulsion Laboratory for their understanding and encouragement; and Dr Peter Torvik for his patience. Also I wish to extend my deepest appreciation to my wife, who showed me infinite patience, to my children, Patrick and Abby, who were very much a part of this study, and to my Lord, Jesus Christ, who kept me going on this project.

Bryan S. DeHoff

Contents

List of Figures

List of Tables

Nomenclature

This list defines only those symbols used in equations or tables in this report. Units listed are used throughout this investigation, unless otherwise specified in the text.

Symbol	Definition	Units
A,B	Fluid dependant constants in Eq 10	
B	Frequency dependant friction damping factor	
ber( )	Real part of Thompson or Kelvin function	
bei( )	Imaginary part of Thompson or Kelvin function	
C	Compliance	psi/cis
c	Acoustic wavespeed	in/sec
D,E,F	Constants in Eq 9	
G	Linearized valve gain, nP_s/Q_s	in/sec
g_c	Gravitational constant, 32.2	$\dfrac{lb_m ft}{lb_f sec^2}$
ID	Internal Diameter	in
J( )	Bessel functions	
j	Complex operator	
k	Ratio of specific heats	
LPRESS	Pump Inlet Pressure	psig
l	Length	in
P	Pressure	psi
Q	Flow rate	cis
R	Absolute temperature	R
r	Internal radius	in
T	Temperature	F
TC	Temperature Correction, $560/(460+T)$	
V	Volume	in^3

Nomenclature (cont)

Symbol	Definition	Units
Z	Impedance	psi/cis
z	complex expression, $x+jy$	
α	Frequency function	
β	Bulk Modulus	psi
θ	Phase angle	deg
μ	Absolute viscosity	lbm/ft-sec
ν	Kinematic viscosity	in^2/sec
ρ	Density	lb-sec^2/in^4
σ	Pressure correction factor, Eq 9	
ω	Frequency	rad/sec

Subscripts	Definition
g	Gas
l	Liquid
o	Standard atmospheric pressure conditions
s	Steady state conditions
1	First order

Abstract

This investigation applies the Hydraulic System Frequency Response (HSFR) computer program to a liquid propellant feed system analysis. During this investigation, the HSFR program was used to predict the oscillatory pressure, flow and impedance conditions existing in an experimental Saturn V first stage LOX suction duct. When necessary to model this system, additional capabilities were added to the program during this investigation. The results from the HSFR analysie are compared to previously published experimental and analytical data for this system. In this comparison, the HSFR program computed resonant frequencies which were between 0 and 3.6% higher than the test data. The sensitivity of the results to changes in the input model was also investigated. The results from this investigation indicate that the theoretical approach of the HSFR program is valid for large diameter feed systems, and recommendations for further model improvements are made.

I. Introduction

Background

Throughout the course of the space program, a recurring problem was encountered during the development of nearly every liquid rocket engine: the problem of combustion instability. In many of the early development programs, the presence of a this problem was not detected until after a catastrophic failure of the engine hardware during a firing. In one program, the nozzle was cut cleanly in two at the throat by combustion instability effects. While not all combustion instability problems manifest themselves in such a destructive manner, the detrimental effects on the engine performance may still jeopardize the success of the mission (Ref 1: 14-16).

Combustion instability problems have been grouped into three classifications: low, intermediate and high frequency instabilities. Both low and intermediate frequency instability problems are frequently caused by wave motion occurring in the propellant feed system (Ref 1: 17,19). This wave motion is in the form of frequency dependent oscillations of the propellant flow rate and pressure about the mean value. While high frequency combustion instability is not directly coupled to the dynamics of the feed system, it is occasionally coupled to an intermediate frequency instability. An additional instability caused by the wave motion in the feed system is a low frequency structural instability referred to as "pogo". Pogo instability is a coupling of the pressure oscillations at the pump inlet and the vibrational modes of the vehicle structure (Ref 1: 17). Operating in a feedback effect, the pressure oscillations are transferred through the engine thrust to drive the longitudinal vibrations of the structure which in turn vibrate the feed system. Should any of the resonance frequencies of the vehicle structure be excited by this vibrational energy, the resulting longitudinal vibration can become strong enough to shake the vehicle apart.

Efforts to understand or predict the occurrence of combustion instability have frequently made use of fluid dynamic models which were developed for pneumatic or hydraulic systems. For example, Holster and Astleford (Ref 2) developed a generalized analytical model and related computer program (Ref 3) which are based on the linearized fluid flow equations developed by D'Souza and Oldenburger (Ref 4).

In the effort to model the pogo phenomenon, Ruben (Ref 5) used both fluid dynamic theories and electrical circuit analogies. He described the stability of the interaction between the structural vibration modes and the propellant feed system by means of forward-loop and feedback transfer functions and Nyquist stability plots. Rubin's model, which does not require the use of a computer to obtain a solution, is still in use today as an engineering design tool.

In the past few years most of the Air Force sponsored work has been in pressure fed engines, and there has been very little activity in the related feed system dynamic problems of pump fed liquid rocket engines. A recent development in the combustion instability area for pressure fed engines is the Transient Performance Program (TPP) (Ref 6). TPP is a multi-purpose, analytical tool for the complete combustion analysis of pressure fed, noncryogenic liquid rocket engines. The feed system subprogram in TPP is capable of describing the propellant feed system dynamics in both transient and steady state operations. Limitations of TPP are that it can not handle pump fed propellant systems, and the input data requires a detailed design of the feed system and thrust chamber. Significant disadvantages of TPP as an engineering design tool are its size and complexity. For a typical TPP analysis problem, such as the Luner Module Ascent Engine, the program will produce 150 to 200 pages of printed output and the execution time on a CDC Cyber 176 would be 5 to 9 computer minutes (Ref 6:36). Limiting the program to just the feed system analysis does not reduce the input data requirements or the execution time significantly.

While there has been very little work in the pump-fed rocket area in the past few years, a project in hydraulic system fluid dynamics was recently completed. In the Aircraft Hydraulic Systems Dynamic Analysis Project (Refs 7,8), the McDonnell Aircraft Company developed four digital computer programs for simulating aircraft hydraulic systems under dynamic conditions. This work was accomplished under contract to the Aero Propulsion Laboratory of the Air Force Wright Aeronautical Laboratories. One of these four programs simulates and predicts the oscillatory flow and pressure occurring in a hydraulic system during steady state operation. This prediction is accomplished with the Hydraulic System Frequency Response program (HSFR) (Refs 9, 10), which will also predict the resonant frequencies, the magnitude of the oscillations at those frequencies and graphically illustrate both these results and the standing pressure waves existing in the system. A feature of HSFR is that it is organized as a tool for the system designer, and system changes are made very easily. The HSFR program, discussed in more detail in Section II, is based on the distributed parameter model of D'Souza and Oldenburger (Ref 4), which was also used in Holster and Astleford's (Ref 2) liquid propellant model. Hillman, et al (Ref 11) also used a distributed parameter approach in developing a linearized impedance model for liquid rocket applications.

The distributed parameter approach to modeling hydraulic networks is based on electrical transmission line theory, and uses the terminology of resistance R, capacitance or compliance C, and inertance L; which are analogous to the electrical terms of resistance, capacitance, and inductance, respectively. In the fluidic definitions for these transmission line parameters, developed by Rohmann and Grogan (Ref 12), the system pressure corresponds to the voltage and the volumetric flow rate corresponds to current. The fluid capacitance and compliance are synonymous, with compliance used by Hillman and capacitance used in HSFR. This investigation will use the term compliance to maintain consistency with Hillman.

The advantage of applying the transmission line terminology and theory to a fluid line is that, in electrical transmission line theory, the impedance, defined as the ratio of the voltage and current, is a function of the resistance, inductance, capacitance and frequency of the electrical circuit. Rohmann and Grogan developed definitions of the fluid system characteristics which are analogous to the electrical circuit characteristics of resistance, inductance and capacitance, and demonstrated that the resulting hydraulic impedance theory would accurately predict the frequency response of a fluid system (Ref 13). The development of this hydraulic impedance theory allowed a large amount of electrical transmission work to be applied to the fluid transmission field.

The fluid dynamic behavior predicted by HSFR is the same as that described in the discussions of pogo and feed system coupled combustion instability (Ref 2: 180). Thus, if the HSFR program can be successfully applied to the analysis of pump-fed liquid propellant feed systems, then the liquid system design analyst will have an additional tool to predict the dynamic behavior of the feed system.

Objective

The objective of this investigation is to determine the applicability of the HSFR program to the analysis of liquid rocket engine feed systems.

Approach

This investigation will evaluate the applicability of the HSFR program to predicting the frequency response of liquid propellant feed systems. An experimental propellant feed system, which has been described by Hillman, et al (Ref 11), will be analyzed by the HSFR program and the frequency response results from the HSFR analysis will be compared with those reported by Hillman. Modifications to the HSFR program will be made when necessary to model the experimental propellant system. These modifications will be in the areas of the input data requirements, fluid property computations, and output options. Where possible, these modifications will provide additions to existing HSFR procedures or capabilities, rather than replacing the original capabilities. A sensitivity study of the HSFR program in the liquid rocket application will be conducted.

II. The Problem

The Experimental Propellant System

The experimental propellant feed system used in this investigation is the S-IC stage LOX suction duct for the Saturn V launch vehicle, as described by Hillman (Ref 11). The Hillman paper describes frequency response tests conducted on this suction duct, using water as the test fluid. Test data and analytical results are presented for two steady state pressures both with, and without through flow. The test data and the system configuration data were previously reported by Brod, et al (Ref 13) during the LOX suction duct dynamic test program, which provided additional configuration data for the sensitivity study of this investigation.

The configuration of the suction duct, together with the configuration data, is shown in Fig 1 (Ref 11:190-192). The LOX prevalve accumulator mentioned in the configuration data is a visor valve and cavity which is pressurized with helium (Fig 2). The compliance of this accumulator was computed from the definition of compliance for a gas C_g, and data from the engineering drawings (Ref 11:191). The compliance for the pump inlet cavitation bubble, reported in Fig 1 was determined empirically (Ref 11:191). This lumped compliance is used to account for the localized fluid column softness caused by the cavitation field of the LOX pump inducer. The reported impedance values at the pump inlet boundary condition were nearly infinite for the zero mean flow condition, and 2.12×10^{-3} psi/cis for the tests with 60 ft^3/sec mean flow (Ref 11:192).

The Hillman paper reports the linearized impedance model results for this LOX suction duct as a plot of the impedance magnitude and phase angle versus frequency at the 90 psia test condition. The impedance model results are reported in Ref 11 for the pump inlet or line 15 on Fig 1 (Ref 11:191). In addition, normalized pressure wave plots are reported for both flow conditions (Ref 11:192).

6

HILLMAN'S CONFIGURATION DATA (Ref 11:190)

LINE DATA

LINE NO	LENGTH (in)	I.D. (in)	WAVE SPEED (in/sec)
1	10.0	20.0	30,341
2	295.4	20.0	30,341
3	203.6	20.0	30,341
4	12.5	18.0	33,942
5	7.9	19.7	25,923
6	31.5	18.0	33,942
7	19.3	18.0	45,878
8	19.2	18.0	45,878
9	9.0	18.0	33,942
10	16.3	18.2	See Below
11	17.0	25.5	(PVC Duct)
12	16.3	18.2	↓
13	17.0	18.0	31,505
14	5.0	18.0	52,358
15	47.0	18.0	52,358
16	8.0	4.0	54,143

PUMP INLET PRESSURE DATA

PUMP INLET PRESSURE (LINE 15)	90.0	130.0	psia
CAVITATION ACCUM COMPLIANCE	2.0	0.9	psi/cis
PREVALVE ACCUM VOLUME	2.1	2.1	ft^3
PREVALVE ACCUM COMPLIANCE	24.7	17.5	psi/cis
PRESSURE VOLUME COMPENSATOR (PVC) DUCT WAVE SPEED			
LINES 10 & 12	8180	6600	in/sec
LINE 11	6990	6690	in/sec

SYSTEM DATA

PUMP INLET IMPEDANCE:
NO FLOW   .00212 psi/cis
WITH FLOW   999,000 psi/cis

FLUID PROPERTIES:
BULK MODULUS   305,000 psi
DENSITY 9.355×10^{-5} lb-sec^2/in^4

Fig 1.
Experimental Propellant System Configuration

Fig 2. LOX Prevalve Accumulator Configuration

The HSFR Program

The Hydraulic System Frequency Response (HSFR) program is organized in a modular form, with a main program calling special subroutines necessary for the dynamic analysis of a hydraulic system (Fig 3). The hydraulic system being analyzed is represented in HSFR by breaking it up into elements, where the elements are various components used in aircraft hydraulic systems (Fig 4). Subroutines in the program are available to model three acoustical sources and six types of hydraulic devices. Acoustical sources modeled are a rotating axial piston pump, a vane pump, and a hydraulic motor. The six types of devices modeled are: lines, volume elements, valves, resonators, piston accumulators, and tee branches. Utility subroutines generate the plots used to display the program's output, and compute the values of the fluid's mass density, kinematic viscosity and bulk modulus at the specified system operating temperature and pressure.

8

```
┌─────────────────────────────────────────────────────────┐
│                                                         │
│        ┌──────────────────────────────────────┐         │
│        │ Specification and Data Statements    │         │
│        │ Read General Input Data              │         │
│        └──────────────────────────────────────┘         │
│                          │                              │
│                          ▼                              │
│        ┌──────────────────────────────────────┐         │
│        │ Call FLUID* for Outlet and Inlet*    │         │
│        │     Pressures                        │         │
│        │ Write Fluid Properties               │         │
│        └──────────────────────────────────────┘         │
│                          │                              │
│                          ▼                              │
│        ┌──────────────────────────────────────┐         │
│        │ Read and Write Input Physical        │         │
│        │     Data System Description          │         │
│        │ Read and Write Output Plot           │         │
│        │     Requirements                     │         │
│        │ Initialize Variables                 │         │
│        └──────────────────────────────────────┘         │
│                          │                              │
│                          ▼                              │
│        ┌──────────────────────────────────────┐         │
│        │ Calculate Fundamental Harmonic       │         │
│        │     Frequency                        │         │
│        └──────────────────────────────────────┘         │
│                                                         │
│        ┌───────────────────────────┐  ┌──────────────┐  │
│        │ Calculate Transfer Matrix │  │ Repeat for   │  │
│        │   for each Circuit        │  │ each         │  │
│        │   Component*              │  │ Harmonic up  │  │
│        │ Calculate Input Impedance │  │ to and       │  │
│        │   at each Component from  │  │ Including    │  │
│        │   Termination Back to Pump│  │ Selected     │  │
│        │                           │  │ Harmonic     │  │
│        └───────────────────────────┘  └──────────────┘  │
│  ┌──────────┐                                           │
│  │ Repeat   │  ┌──────────────────────────────────────┐ │
│  │ for      │  │ Call PUMP                            │ │
│  │ Each Pump│  │ Calculate Input Pressure and        │ │
│  │ Speed    │  │   Flow for each Component           │ │
│  │ over     │  └──────────────────────────────────────┘ │
│  │ Range    │                                           │
│  └──────────┘  ┌──────────────────────────────────────┐ │
│                │ Calculate Energy Density and        │ │
│                │   Intensity and Store with          │ │
│                │   Flow, Pressure and Impedance      │ │
│                └──────────────────────────────────────┘ │
│                ┌──────────────────────────────────────┐ │
│                │ Plot Values of Selected Param-      │ │
│                │   eters* at Selected Locations      │ │
│                │   vs Pump Speed                     │ │
│                │ Plot Standing Waves*                │ │
│                └──────────────────────────────────────┘ │
│                * Signifies Areas Changed                │
│                                                         │
└─────────────────────────────────────────────────────────┘
```
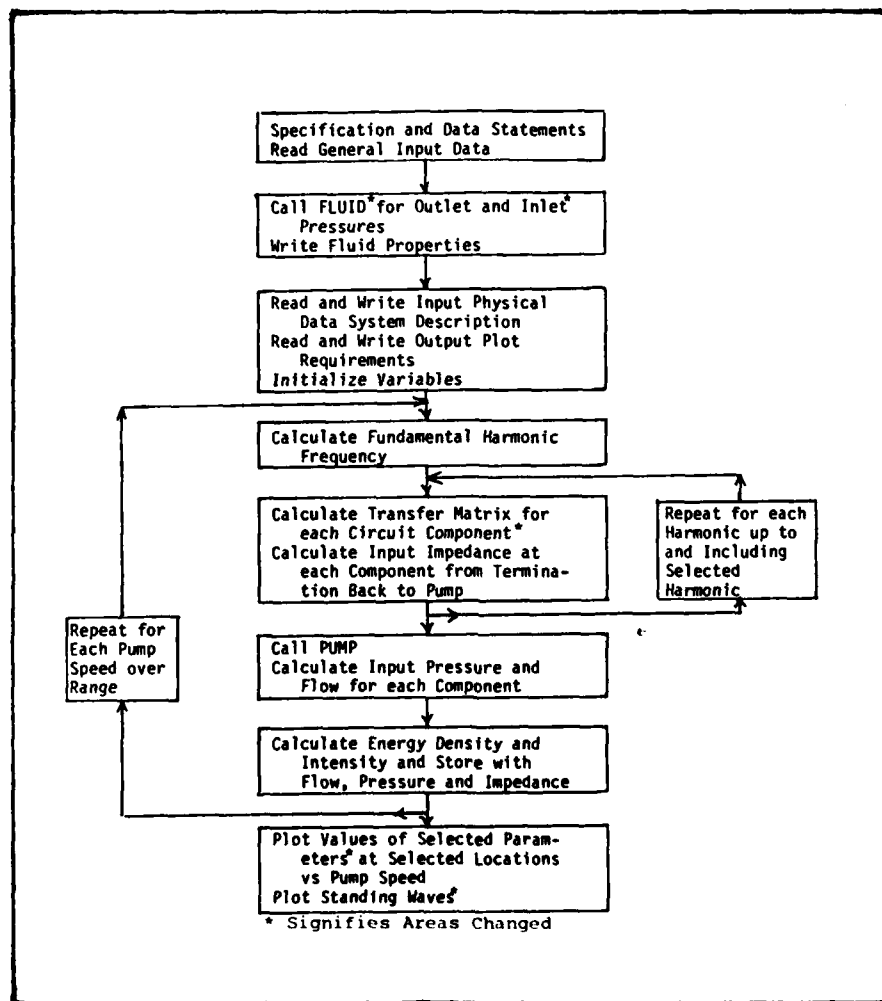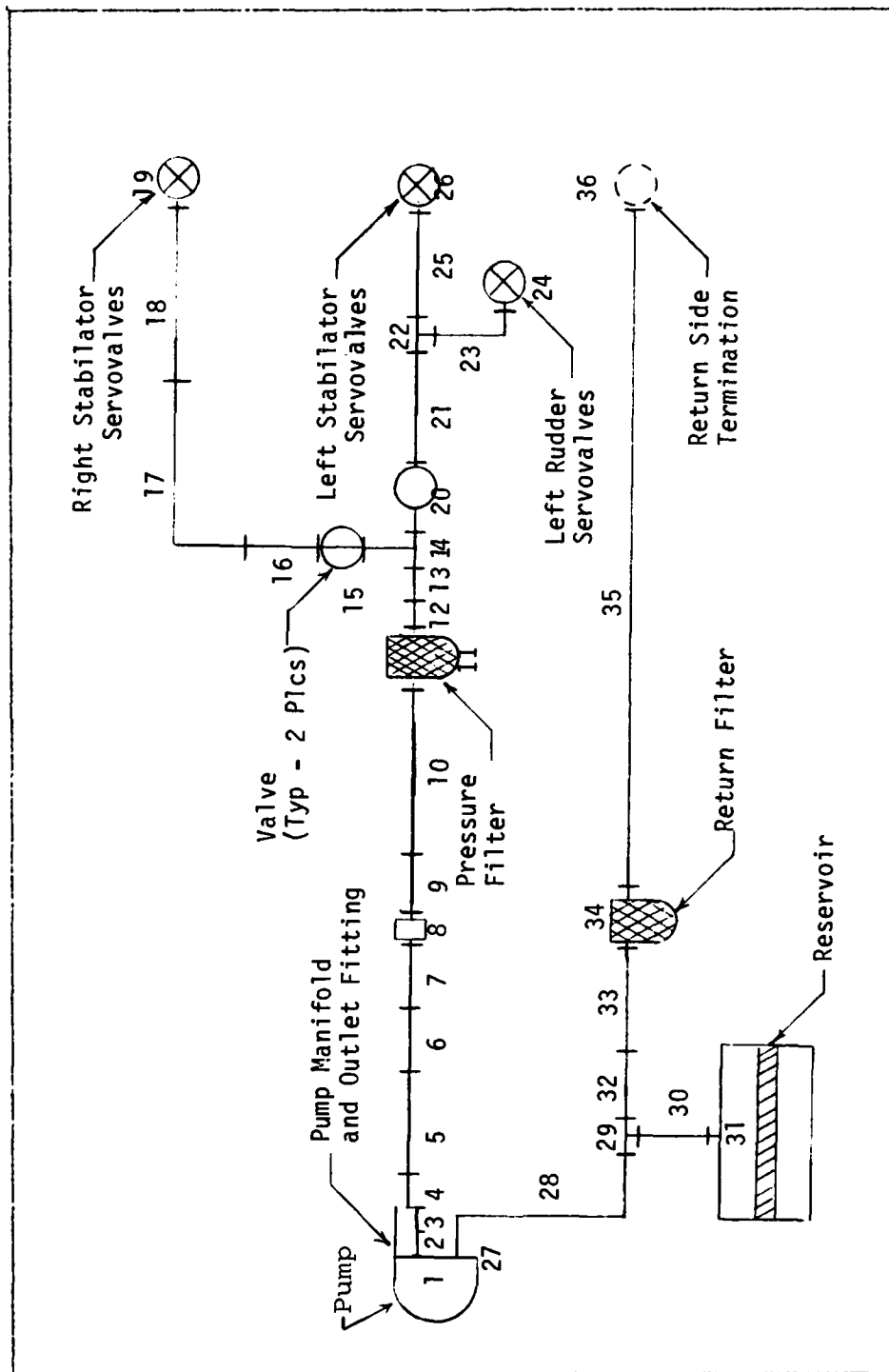
Fig 3. HSFR Main Program Flow Chart

9

Fig 4. Typical Hydraulic System Model for HSER Analysis (Ref-9: Sec 2,3)

During this investigation the FLUID subroutine in HSFR, which computed the kinematic viscosity, density, and bulk modulus for three different types of hydraulic oils, was rewritten using the same programming approach of the original subroutine, to compute the same three properties for three storable liquid propellants and water, the fluid used in Hillman's work (Ref 11). The fluid properties are computed at the steady state temperature and pressure for both the high pressure side and the low pressure, or return side of the system, based on tabulated fluid property data or empirical equations. The new subroutine, which completely replaces the original HSFR FLUID subroutine for hydraulic oils, contains fluid property data as a function of temperature, and when available, pressure, for: RP-1, a kerosene-like fuel; Monomethyl Hydrazine (MMH), a fuel; nitrogen tetraoxide (N_2O_4), an oxidizer; and water, a test fluid. The input instructions for this new fluid subroutine are given in Appendix A, and the data used in the subroutine are discussed in detail in Appendix B.

The HSFR program results for flow, pressure and impedance calculations are plotted as the magnitude of the complex flow, pressure and impedance versus pump shaft speed. At the user's request, the total acoustic energy density and acoustic intensity are computed and plotted versus pump speed for specified elements in the system. Standing wave plots of the pressure amplitude versus the physical location of each element in the system can be output for either specified pump speeds, or for all pump speeds where the pressure amplitude exceeds a specified input value. The capability of plotting two additional items, the phase angle and pressure gain, was added to the HSFR program during this investigation. The phase angle, in degrees, is the angular difference between the complex pressure and complex flow. The pressure gain in decibels is plotted between any two elements in the system, and the user may request a maximum of ten gain plots of the system.

The modeling theory and organization of the program are discussed in the HSFR Technical Manual (Ref 10), and instructions for describing a system and using the

11

program are in the User's Manual (Ref 9). While the procedure for obtaining the standing wave plot is not discussed in the program manuals, user's instructions were developed as a part of this investigation. These instructions, and those for the phase angle and pressure gain plots, are given in Appendix A.

The studies to verify the accuracy of the HSFR predictions, which were done as part of the Air Force contract, were reported by McDonnell Douglas (Refs 7, 8). The accuracy in the frequency prediction ranged between 0 and 2%, and the pressure amplitude predictions ranged from 0 to 30% high (Ref 7:64). Additional studies of the HSFR program were accomplished at the Air Force Institute of Technology (Refs 14 - 16), with similar accuracies reported in those studies. All the verification studies with HSFR have been done on the high pressure side of the hydraulic system, downstream of the pump. However, the project documentation states: "Resonance frequency predictions in the return system should be reasonably good, owing to the use of the same computation method and models as are used for pressure system analysis. The accuracy of predicted pressure amplitude at return system resonances is unknown." (Ref 7:98) This is important to this investigation, because the analysis of propellant feed system dynamics will require modeling the majority of the feed system as a return or suction system in the HSFR code.

The Modeling Theory

This investigation is concerned with accurately representing the experimental propellant system described by Hillman (Ref 11) for analysis with the HSFR program. Since the data published by Hillman will be used to verify the HSFR results, both Hillman's model and HSFR need to have compatible definitions. The hydraulic impedance Z, is equivalently defined as the ratio of the complex pressure and complex flow at any location x, in both models (Ref 10: Sec 3, 16 and Ref 11: 190).

The configuration data reported by Hillman includes the compliance of two elements in the propellant system: the LOX prevalve accumulator and the pump inlet cavitation region. The compliance of a fluid element is primarily the effect of the compressibility of the fluid in that element, which varies considerably for liquid and gas filled elements. For liquid filled systems, the compliance is a function of the volume and the fluid's bulk modulus:

$$c_1 = \frac{V}{\beta} \tag{1}$$

The VOLUME subroutine in the HSFR program used Eq 1 to model components such as filter cavities or reservoirs. For gas filled systems like the LOX prevalve accumulator, the compliance is based on the ratio of specific heat for the gas, the system steady state pressure, and the volume (Ref 12: 857):

$$c_g = \frac{V}{kP_s} \tag{2}$$

The LOX prevalve accumulator described by Hillman is a helium filled volume, and the reported compliance is based on the gas definition of Eq 2. During this investigation, the VOLUME subroutine was modified to include Eq 2 as an optional computation for the compliance of a gas filled volume such as the LOX prevalve accumulator. The modified subroutine will also accept an empirically determined

13

compliance as input data; an option which was used to model the pump inlet cavitation region for the Hillman comparisons. The instructions for this additional input data are provided in Appendix A. Because the HSFR program treats volumes as lossless elements, no pressure or flow losses are computed for a volume element. In terms of the impedance theory, there is no resistance or inertance in a volume, just compliance. The pressure and flow losses are handled by the LINE subroutine, which must be used for any inlet line segments in the volume element.

In modeling the pressure and flow relationship in a line segment, the HSFR program uses an approximation of the frequency dependant friction damping factor B, defined by D'Souza and Oldenburger (Ref 4). The definition of B in D'Souza and Oldenburger is based on the Thomson functions of zero order and their derivatives, according to Eq 26 of Ref 4. However Eq 26 of Ref 4 is derived from the following (Ref 4:592):

$$B = \frac{1}{\left[-\frac{2}{\alpha j^{\frac{1}{2}}} \frac{J_1(-\alpha j^{\frac{1}{2}})}{J_0(-\alpha j^{\frac{1}{2}})} - 1 \right]^{\frac{1}{2}}} \tag{3}$$

where
$$\alpha = r\left(\frac{\omega}{\nu}\right)^{\frac{1}{2}}$$

and substituting
$$-j^{\frac{1}{2}} = j^{\frac{3}{2}}$$

Replacing the Bessel functions, which contain complex arguments, with Kelvin functions of real arguments gives:

$$B = \frac{1}{\left[-\frac{2}{\alpha j^{\frac{1}{2}}} \frac{ber_1(\alpha) + bei_1(\alpha)}{ber(\alpha) + bei(\alpha)} - 1 \right]^{\frac{1}{2}}} \tag{4}$$

where ber and bei are Kelvin functions of the first kind. D'Souza and Oldenburger referred to ber and bei as Thomson functions, but Ref 17 referred to them as Kelvin functions. The equivalency of the titles is shown in Appendix C.

Because of the awkward and inefficient nature of using tabulated Kelvin functions in a computer program, HSFR approximated Eq (4) by (Ref 10:Sec 5,1):

$$B = 4\left(\frac{1}{\sqrt{2}\,\alpha}\right)^2 - \frac{1}{\sqrt{2}\,\alpha} + j\left(\frac{1}{\sqrt{2}\,\alpha} - 1\right) \tag{5}$$

This approximation introduced an error of less than one percent over the frequency range of interest during the development of the HSFR program (Ref 10: Sec 5,2). However, when using HSFR in the analysis of an aircraft antiskid system, the Boeing Commercial Airplane Company obtained erroneous results for the system undergoing low frequency pressure oscillations (Ref 18). Boeing determined that the B approximation in HSFR was the source of the error, and replaced the approximation with a new one, based on Trikha's work (Ref 19):

$$B = \left(-1 + j\frac{8}{\alpha^2} - 4\left(\frac{40}{8000+j\alpha^2} + \frac{8.1}{200+j\alpha^2} + \frac{1.0}{264+j\alpha^2}\right)\right)^{\frac{1}{2}} \tag{6}$$

This approximation is ideal for low frequency applications, correcting the significant discrepancies of the HSFR approximation. Figure 5 shows the agreement of both the real and imaginary parts of Eq 6 with the results of D'Souza and Oldenburger's exact solution, Eq 4, and divergence of the real and imaginary parts of the HSFR approximation, Eq 5 from the exact solution when the frequency function α, is less than 4. According to information received from Hillman (Ref 20), Boeing recommended that the approximation of Eq 6 be used in place of Eq 5 and the Aero Propulsion Lab accepted their recommendation. Equation 5 was replaced with Eq 6 for the analyses done on the experimental propellant system. However this replacement had no effect on the results because the frequency function α in Hillman's system (Ref 11) ranges from 860 to 3050 for the frequency range used. As Fig 5 shows, the HSFR approximation agrees with the exact solution at this range of frequency functions.
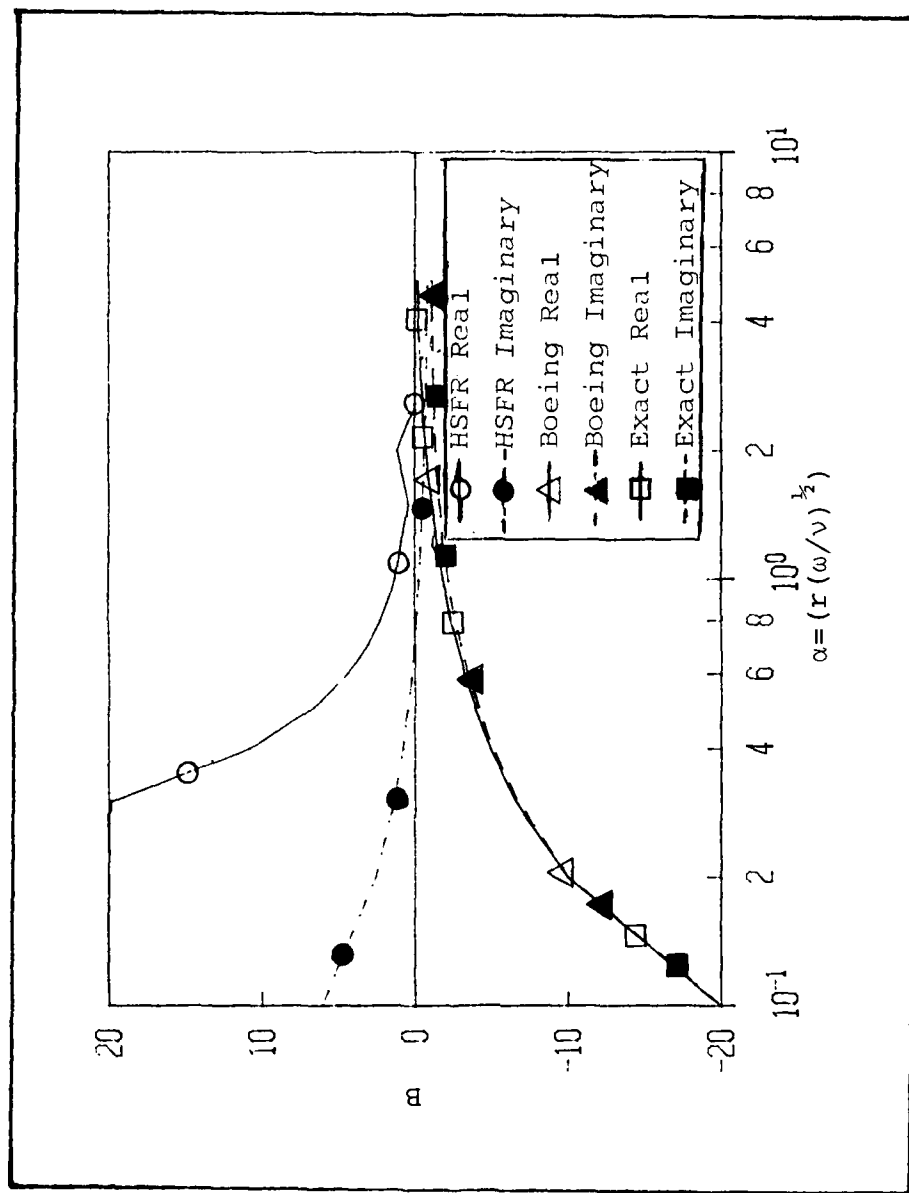
Fig 5. Comparison of B Approximations

16

III. Procedure

Representing the Experimental Propellant System

For analysis with the HSFR program, the experimental propellant system was modeled as a suction side of a system. The configuration data reported by Hillman (Ref 11), discussed earlier (Fig 1), provided most of the input data needed to model the physical system. Additional data on the physical characteristics of the propellant feed system were obtained from Brod (Ref 13) and from conversations held with Mr H.F. Hillman during this investigation (Ref 20).The propellant system model is shown schematically in Fig 6, and additional description data are provided by Table I.

The configuration data for the line elements of the propellant system reported an acoustic wavespeed, which is corrected for the effects of the duct wall, and an inside diameter for each section of the suction duct (Ref 11:190). Prior to this investigation, the LINE subroutine of the HSFR program used the fluid density and bulk modulus and the suction duct's modulus of elasticity in computing the corrected wavespeed. Because the wall thickness and modulus of elasticity were not provided by Hillman, the LINE subroutine was modified as part of this investigation to accept the inside diameter and corrected wavespeed data, which were reported by Hillman, as an option to having the subroutine make the wavespeed correction. The instructions for using this optional input data format are given in Appendix A.

In modeling the propellant system for analysis with HSFR, the acoustical source described by Hillman could not be modeled with HSFR. The experimental system, as used by Hillman (Ref 11), contained a 4 in diameter bleed flow line coming off of the main suction duct some distance above the location of the LOX turbopump inlet in a flight system (Fig 1, line 16). The bleed flow discharging through the pulsating valve on the end of this four in line created cyclic pressure and flow waves in the main duct. Two problems were encountered when modeling this configuration for analysis with
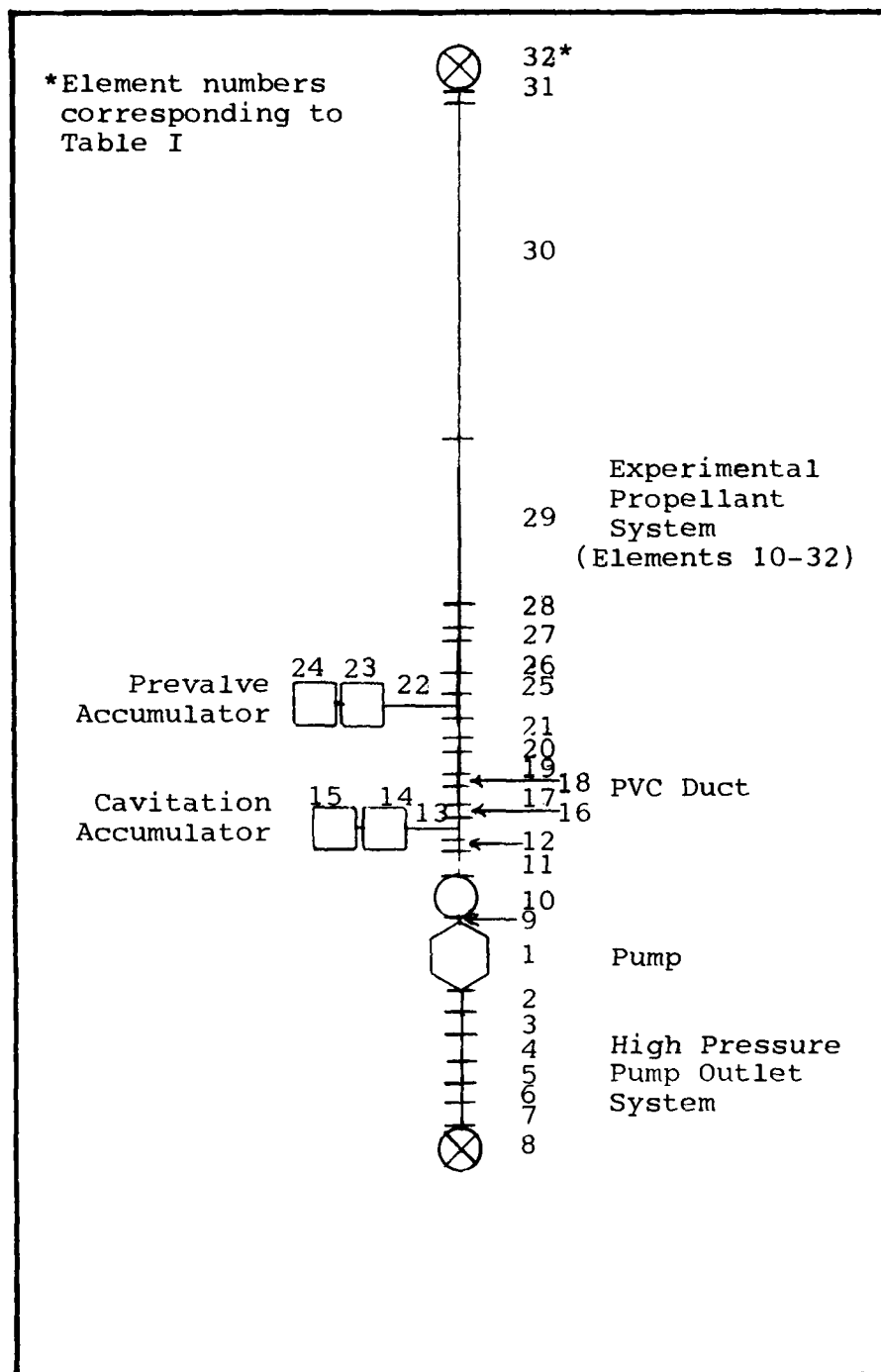
17

*Element numbers
corresponding to
Table I

32*
31

30

Experimental
Propellant
System
(Elements 10-32)

29

28
27
26
25
Prevalve   24 23   22
Accumulator
21
20
19
18 PVC Duct
Cavitation   15 14   13   17   16
Accumulator   12
11
10
9
1   Pump

2
3
4   High Pressure
5   Pump Outlet
6   System
7
8

Fig 6.
HSFR Model of Experimental Propellant System

18

Table I.

System Data for HSFR Representation

```
SYSTEM DATA
    STEADY STATE TEMP: 50F        FLUID: WATER
    NUMBER OF PISTONS: 9
    PUMP SPEED: 8 - 200rpm  SPEED INCREMENT:2
```

```
LINE DATA
    ELEMENT
    NUMBER   LENGTH   ID    WAVESPEED
    (FIG 6)  (in)     (in)  (in/sec)

    PUMP OUTLET SYSTEM LINE DATA
```

ELEMENT NUMBER (FIG 6)	LENGTH (in)	ID (in)	WAVESPEED (in/sec)
2	10.	20.	30341.
3	10.	20.	30341.
4	10.	20.	30341.
5	10.	20.	30341.
6	10.	20.	30341.
7	10.	20.	30341.

EXPERIMENTAL PROPELLANT SYSTEM LINE DATA

ELEMENT NUMBER	LENGTH (in)	ID (in)	WAVESPEED (in/sec)
11	47.	18.	52358.
12	5.	18.	52358.
16	17.	18.	52358.
20	9.	18.	33942.
21	19.2	18.	45878.
25	19.3	18.	45878.
26	31.5	18.	33942.
27	7.9	19.7	25923.
28	12.5	18.	33492.
29	203.6	20.	30341.
30	295.4	20.	30341.

```
PUMP ELEMENT: ELEMENT NUMBER 1. DATA
PROVIDED BY HSFR USER'S MANUAL
(Ref 9: Sec 2, 43-48)
```

PRESSURE VOLUME COMPENSATOR DUCT DATA @90psi

ELEMENT NUMBER	LENGTH (in)	ID (in)	WAVESPEED (in/sec)
17	16.3	18.2	8180.
18	17.	25.2	6990.
19	16.3	18.2	8180.

VALVE DATA USED FOR TERMINAL IMPEDANCE

ELEMENT NUMBER	VALVE GAIN (psi/cis)	THROUGH FLOW (cis)
8	See Tables II -VI	See Tables II - VI
10	"	"
32	0.0	103680.

CAVITATION ACCUMULATOR DATA

ELEMENT NUMBER	DESCRIPTION
13	Tee Branch Element
14	1st Stage Volume Element See Data in Tables II - VI
15	2nd Stage Volume Element See Data in Tables II - VI

LOX PREVALVE ACCUMULATOR DATA

ELEMENT NUMBER	DESCRIPTION
22	Tee Branch Element
23	1st Stage Volume Element See Data Tables II - VI
24	2nd Stage Volume Element See Data Tables II - VI

HSFR. First, there is no model of a variable area orifice available for HSFR; and second, the HSFR program cannot handle flow out of both the main duct and the pulsating valve branch. The program requires the acoustic source to be the only exit from an inlet system and the only entrance to a pressurized system (Fig 7). If the HSFR representation of the experimental propellant system included the bleed flow line, the program would treat that line (Line 16, Fig 1) as the main line and the portion of the suction duct below the bleed flow line as a short branch off of the main flow path. In order to prevent this erroneous modeling, the propellant system configuration used in this investigation does not include the pulser branch used in the experimental propellant system, and instead, has the pump model located at the end of the suction duct as would be expected in a flight system. The pump model used is of a pressure compensated, rotating, axial nine piston hydraulic pump. The input data for this model was obtained from the HSFR User's Manual (Ref 9: Sec 2, 43-48).

Modeling the two lumped compliances in the LOX suction duct; the LOX prevalve accumulator and the pump inlet cavitation region, required the addition of the capability for computing the compliance of a gas filled volume in the VOLUME subroutine of HSFR discussed earlier. In preparing the input data for a volume, the HSFR Technical Manual states that any inlet or outlet lengths associated with the volume element should be modeled as line elements (Ref 10: Sec 6,2). The configuration data in Fig 1 (Ref 11:190), includes the line lengths associated with the prevalve accumulator and cavitation region, and the placement of these elements on branches of the main line was confirmed by Hillman during this investigation (Ref 20). Using the modified VOLUME subroutine, the LOX prevalve accumulator was modeled as two volume elements in series on a branch from the main line, with a total volume of 3628.8 in^3. Two elements were used to allow a variation in the gas volume, with a volume of water occupying any accumulator volume not filled with helium. The gas volume was varied in the sensitivity study portion of this investigation. For certain
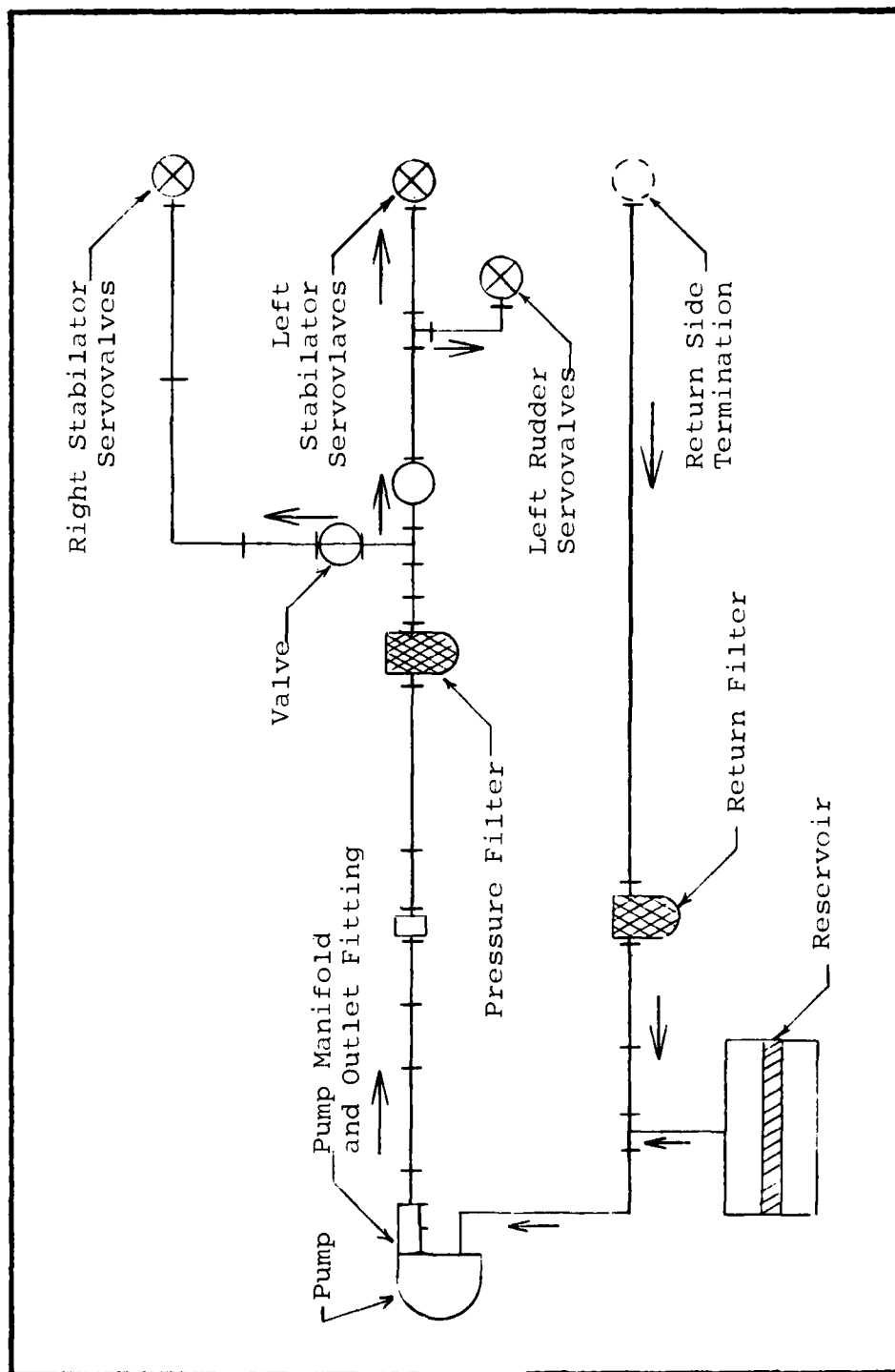
20

Fig 7. Modeling Flow Directions with HSFR

21

configurations the compliance value reported by Hillman was used to model the prevalve accumulator, instead of the physical dimensions. The cavitation region was modeled two ways. For comparison with Hillman's results, the cavitation region was modeled as a single volume element on a branch off the main line, and described by the empirically determined compliance reported by Hillman (Ref 11:190). For the sensitivity study, two volume elements were used to provide for variation in the gas and water volume using physical dimensions obtained from Brod (Ref 13:13).

The configuration data reported by Hillman (Fig 1) lists a line element as the upper end of the propellant system and mentions a pressurized water tank in the system description (Ref 11:190-191). However, Brod (Ref 13:3) reports that the ullage pressure in the water tank was varied during the test runs to maintain a constant steady state pressure condition. To model this constant pressure condition at the upper end of the system, an open valve element was used to set the oscillatory pressure at this end equal to zero. The pressure/flow relationship in a valve is described by the linearized valve gain G, as defined in the nomenclature (Ref 9: Sec 2,26). The gain for the valve at the upper end of the system was set to zero, which implies a constant pressure drop for any flow rate through the valve.

Another valve element was used to represent the main flow control valve shown in Fig 1. The terminal impedance values reported by Hillman for the main flow control valve were nearly infinite for the no-flow condition and 2.12×10^{-3} psi/cis for the 60 cfs through flow condition at 90 psi (Ref 11: 191). For the model used in this investigation, the terminal impedance was modeled by a terminating valve element at the end of the pump outlet system below the pump model in Fig 6 for both the no flow and the 60 cfs through flow condition and by an additional valve element at the pump inlet for the through flow condition. For the no flow condition, the terminating valve gain was 999,000 psi/cis. For the through flow condition this valve gain was 0.019 psi/cis, because the pump outlet side pressure drop was 1000 psi.

22

The Analysis Conditions

In order to determine the applicability of the HSFR program to the analysis of liquid rocket feed systems, the objective of this investigation, the propellant feed system model conditions were varied to compare with previously reported results of Hillman (Ref 11) and Brod (Ref 13). Hillman's results provided a comparison of the pump inlet impedance resonant frequencies, the phase shift frequencies, and the normalized pressure wave shapes in the system at the resonant frequencies. The configuration data used in the HSFR analyses for the Hillman comparisons are in Table II.

The effect of changes in the input conditions on the HSFR program results was investigated by analyzing a series of configurations at pressures which had been previously investigated by Brod (Ref 13). Factors varied individually in this sensitivity study were: the prevalve accumulator gas volume, the gas volume in the cavitation ring, the pump inlet pressure and the system temperature. Aside from the components being analyzed, all components were modeled as shown in Table I.

The effect of the gas volume in the prevalve accumulator was determined by analyzing the propellant system at pump inlet pressures of 58 and 130 psia for five different fractional gas volume levels using the two stage model of the prevalve accumulator. For this comparison, the cavitation ring was modeled as a lumped compliance of 2.0 psi/cis, and the terminating impedance valve gain was at the no flow setting of 999,000 psi/cis. The pressurizing gas was helium, with a specific heat ratio of 1.66. The water and gas volumes for the respective analysis conditions are listed in Table III.

The frequency effect of the cavitation ring gas volume was identified by analyzing the system at a pump inlet pressure of 110 psia, with no gas in the prevalve accumulator, and the terminating valve impedance at the no flow setting of 999,000 psi/cis. This system configuration was analyzed with the gas volume in the cavitation

23

Table II

Configuration Data for Hillman Comparisons

```
CONFIGURATION: 90psia No Flow      Propellant Sys Press: 90psia
   Pump Inlet Press: 75.3psig        Outlet Sys Press: 3000psig
   Resonant Test Press: 0.01psi         Test Bandwidth: 5rpm

   COMPONENT          ELEMENT
   NAME               NUMBER      PARAMETER LIST

   Terminal Imped       8         G= 999,000psi/cis Q= 0.0cis
   Valves              10         Not Used

   Cavitation Accum    14         Not Used
                       15         C= 2.0psi/cis

   Prevalve Accum      23         Not Used
                       24         C= 24.7psi/cis
   ***************************************************************
CONFIGURATION: 90psia,60cfs Flow      Prop Sys Press: 90psia
   Pump Inlet Press: 75.3psig        Outlet Sys Press: 1000psig
   Resonant Test Press: 0.01psi         Test Bandwidth: 5rpm

   COMPONENT          ELEMENT
   NAME               NUMBER      PARAMETER LIST

   Terminal Imped       8         G= 0.019psi/cis Q= 103680.cis
   Valves              10         G= 0.019psi/cis

   Cavitation Accum    14         Not Used
                       15         C= 2.0psi/cis

   Prevalve Accum      23         Not Used
                       24         C= 24.7psi/cis
   ***************************************************************
CONFIGURATION: 130psia,60cfs Flow      Prop Sys Press: 130psia
   Pump Inlet Press: 115.3psig        Outlet Sys Press: 1000psig
   Resonant Test Press: 0.01psi         Test Bandwidth: 5rpm

   COMPONENT          ELEMENT
   NAME               NUMBER      PARAMETER LIST

   Terminal Imped       8         G= 0.019psi/cis Q= 103680.cis
   Valves              10         G= 0.019psi/cis

   Cavitation Accum    14         Not Used
                       15         C= 0.9psi/cis

   PVC DUCT            17         1= 16.3in ID=18.2in c=6600.in/sec
                       18         1= 17.0in ID=25.2in c=6690.in/sec
                       19         1= 16.3in ID=18.2in c=6600.in/sec

   Prevalve Accum      23         Not Used
                       24         C= 17.5psi/cis
```

Table III

Configuration Data for Prevalve Accumulator Sensitivity

```
CONFIGURATION: 130psia No Flow   Propellant Sys Press:130psia
   Pump Inlet Press: 115.3psig      Outlet Sys Press: 3000psig
   Resonant Test Press: 0.01psi        Test Bandwidth: 5rpm
```

COMPONENT NAME	ELEMENT NUMBER	PARMETER LIST
Terminal Imped	8	G= 999000.psi/cis Q= 0.0cis
Valves	10	Not Used
Cavitation Accum	14	Not Used
	15	C= 2.0psi/cis
Prevalve Accum	23	Water Volume See Below*
	24	Gas Vol* P= 130psia k= 1.66

```
- - - - - - - - - - - - - - - - - - - - - - - - - - - - - - - - - - - - - - -
CONFIGURATION: 58psia No Flow              Prop Sys Press: 58psia
   Pump Inlet Press: 43.3psig      Outlet Sys Press: 3000psig
   Resonant Test Press: 0.01psi        Test Bandwidth: 5rpm
```

COMPONENT NAME	ELEMENT NUMBER	PARAMETER LIST
Terminal Imped	8	G= 999000.psi/cis Q= 0.0cis
Valves	10	Not Used
Cavitation Accum	14	Not Used
	15	C= 2.0psi/cis
Prevalve Accum	23	Water Volume See Below*
	24	Gas Volume P= 58.psia k=1.66

```
- - - - - - - - - - - - - - - - - - - - - - - - - - - - - - - - - - - - - - -
```

*VOLUMES USED

% GAS VOLUME	ELE 23 WATER VOL (in^3)	ELE 24 GAS VOL (in^3)
20.	2903.1	725.7
40.	2177.3	1451.5
60.	1451.5	2177.3
80.	725.7	2903.1
90.	362.9	3265.9

ring ranging from zero to fifty percent of the total volume of 1570.0 in^3. The zero gas volume condition used a single stage volume model while all other conditions used a two stage volume model. The pressurizing gas was helium with a specific heat ratio of 1.66, and the system temperature was 50F. The volumes used for each condition are listed in Table IV.

Table IV

Configuration Data for Cavitation Accumulator Sensitivity

CONFIGURATION: 110psia,No Flow,No Gas in Prevalve Accum

Prop Sys Press: 110psia
Pump Inlet Press: 95.3psig   Outlet Sys Press: 3000psig

COMPONENT NAME	ELEMENT NUMBER	PARAMETER LIST
Terminal Imped	8	G= 999000psi/cis Q= 0.0cis
Valves	10	Not Used
Cavitation Accum	14	Water Volume See Below*
	15	Gas Volume* P= 110.0 k= 1.66
Prevalve Accum	23	Not Used
	24	Water Filled V= 3628.8in^3

*VOLUMES USED

GAS/WATER RATIO	ELE 14 WATER VOL (in^3)	ELE 15 GAS VOL (in^3)
0.000	1570.	0.
.016	1545.	25.
.032	1520.	50.
.064	1470.	100.
.127	1370.	200.
.255	1170.	400.
.382	970.	600.
.500	785.	785.

The pump inlet pressure effect was studied on two configurations, one without and one with gas in the prevalve accumulator. The first configuration, which did not contain the cavitation ring or any gas in the prevalve accumulator, was analyzed at pump inlet pressures of 60, 90, 110, and 130 psia. The second configuration had the prevalve accumulator volume filled with helium and used Hillman's reported

compliance for the cavitation ring. This configuration was analyzed at pump inlet pressures of 55, 70, 90, 110, and 130 psia. There was no through flow in either configuration. The element data pertinent to the pressure effect analyses are in Table V and VI for without and with the gas filled prevalve, respectively.

The final sensitivity studied during this investigation was the effect of system temperature. This parameter was not varied in Brod's investigation, but several temperatures were used in the HSFR program during this investigation. System temperatures of 75, 65, 55, and 50 F were used in the analysis of Hillman's 90 psia with flow configuration (Table II).

Table V

Configuration Data for Pump Inlet Pressure Sensitivity
Without Prevalve Accumulator

```
CONFIGURATION: No Cavitation Accum, No Flow
   Prop Sys Press: Varied
   Pump Inlet Press: See Below*      Outlet Sys Press: 1000psig

COMPONENT           ELEMENT
NAME                NUMBER     PARAMETER LIST

Terminal Imped        8        G= 999000.psi/cis Q= 0.0cis
Valves               10        Not Used

Cavitation Accum 13-15         Not Used

Prevalve Accum       23        Not Used
                     24        Water Filled, V= 3628.8in³
----------------------------------------------------------------
*PROP SYS PRESSURES USED

              PROP SYS         PUMP INLET
              PRESS (psia)     PRESS (psig)

                60.              45.3
                90.              75.3
               110.              95.3
               130.             115.3
```

Table VI

Configuration Data for Pump Inlet Pressure Sensitivity
with Prevalve Accumulator

```
CONFIGURATION: No Flow, With Cavitation Accum
  Prop Sys Press: Varied
  Pump Inlet Press: See Below*     Outlet Sys Press: 3000psig

  COMPONENT           ELEMENT
  NAME                NUMBER     PARAMETER LIST

  Terminal Imped        8        G= 999000.psi/cis Q= 0.0cis
  Valves               10        Not Used

  Cavitation Accum     14        Not Used
                       15        C= 2.0psi/cis

  Prevalve Accum       23        Not Used
  Gas Filled           24        V= 3628.8 P= See Below* k=1.66
-------------------------------------------------------------
*PROP SYS PRESSURES USED

              PROP SYS     PUMP INLET       P
              PRESS (psia) PRESS (psig)   (psia)

                55.          40.3           55.
                70.          55.3           70.
                90.          75.3           90.
               110.          95.3          110.
               130.         115.3          130.
```

IV. Results

Hillman Comparison Results

Analytical results previously published by Hillman (Ref 11) for the configurations discussed in Table II were compared with the HSFR predictions for the following: impedance amplitude versus frequency, phase angle versus frequency, distance versus normalized pressure without flow, and distance versus normalized pressure with 60 cfs through flow. For the impedance amplitude and phase angle comparisons, it is important to remember that the different acoustic source models used in the two investigations can be expected to provide different signal amplitudes. The comparable information, then, is the frequency of the amplitude peak and phase angle shift. The pressure wave shape results of Hillman, presented in the form of distance versus normalized pressure, contain information about the phase of the pressure which was not available in the HSFR results, as HSFR plots a standing half wave and does not provide the phase angle data available in a full wave shape plot. In order to compare the HSFR wave shapes with Hillman's, the sign of the normalized pressure was assumed to be the same as Hillman's results.

The HSFR impedance amplitude and phase angle results at the pump inlet location, line 15 in Fig 1, are presented in Fig 8 and Fig 9. Hillman's corresponding results are presented in Fig 10. The HSFR results are plotted for the no flow condition in Fig 8 and with 60 cfs through flow in Fig 9, and are plotted against pump speed in rpm, not frequency. The conversion for the nine piston pump is 0.15 Hz/rpm. Thus, the HSFR results show predicted impedance resonances at 14 rpm (2.1 Hz), 114 rpm (17.1 Hz), and 172 rpm (25.8 Hz), as compared to the resonant frequencies of 2.1, 16.5, and 25.0 Hz identified by the testing as reported by Hillman (Ref 11:192) and Brod (Ref 13:20). There was no difference in the HSFR predicted impedance frequency response for the no flow and the through flow condition. For the second and third
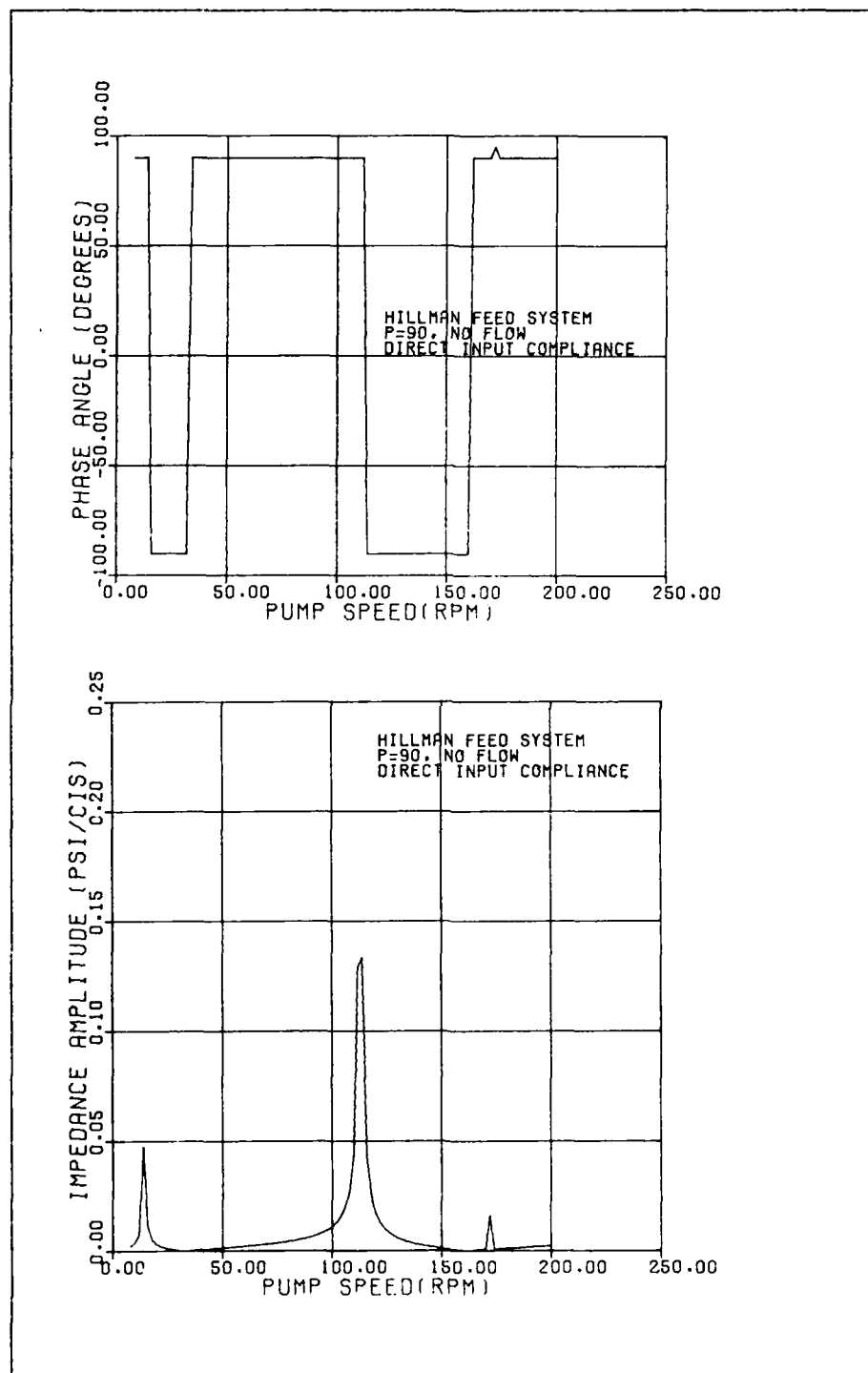
Fig 8.

HSFR Impedance and Phase Angle Results for No Flow
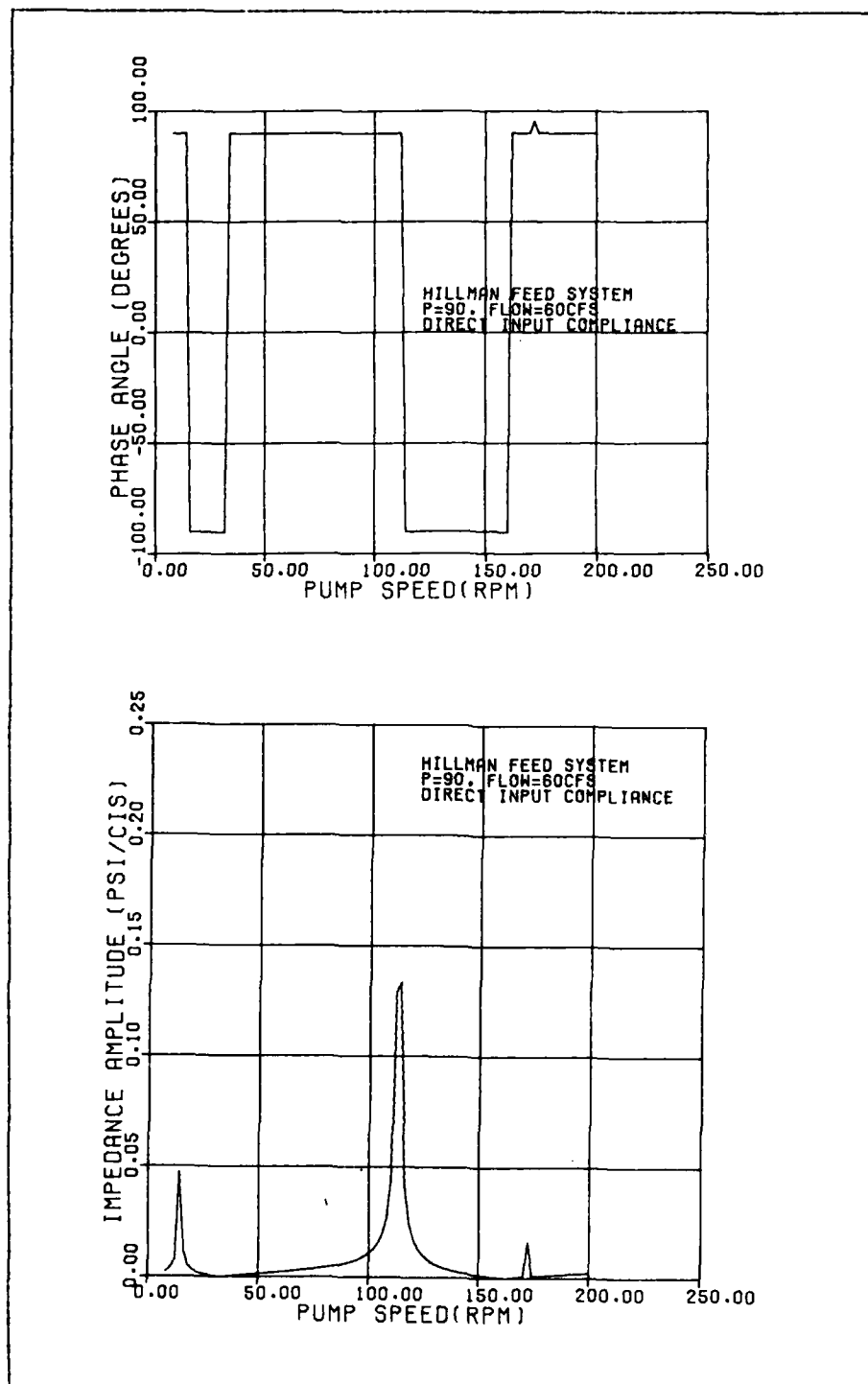
Fig 9.

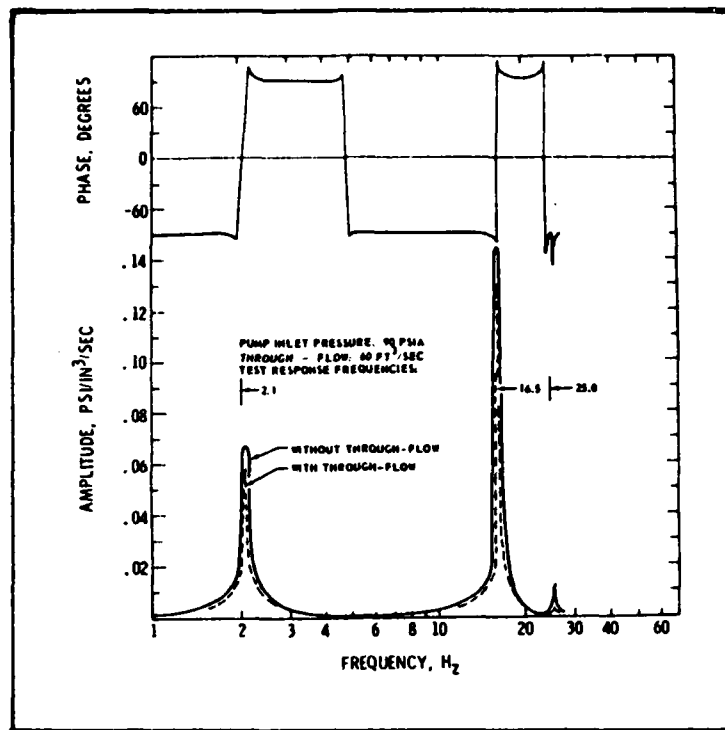HSFR Impedance and Phase Angle Results for 60cfs Through Flow

Fig 10. Hillman's Impedance Model Results (Ref 11:191)

modes, the HSFR program results differ from the test data by 3.6% and 3.2% respectively. In comparing the phase angle plots of Figs 8 and 9, and Fig 10, the the behavior of the phase angle is similar but the sign is reversed. In Hillman's results, all impedance resonances occur at phase angle shifts from -90° to 90°, with the appearance of shifting through 180° instead of 0°. In the HSFR results, all resonances occur when the phase angle shifts from 90° to -90°, also through 180°. The small spikes at the third mode in the phase angle plots of Figs 8 and 9 are resonance related phase angle shifts: the digital results show that at 25.8 Hz the phase angle jumps from 90° to 95°, and at 26.1 Hz the phase angle is again 90°. Hillman's phase angle results also indicate a very transient phase shift at the third mode frequency (Fig 10). Thus the two models, HSFR and Hillman's, agree in the resonant frequency predictions based on impedance, but the predicted initial phase angles are opposite. This discrepancy will be discussed later.

Figures 11 through 14 compare the predicted pressure wave shapes in the feed system at the predicted resonant frequencies. Figure 11 contains the normalized standing pressure waves predicted by Hillman's model and the test data measured during the test program for the no flow condition and Fig 12 contains the results for the 60 cfs through flow condition (Ref 11:192). Hillman reported that the second mode wave shape is taken from a 130 psia pump inlet pressure condition because of the lack of satisfactory data at the 90 psia condition (Ref 11:192). Figures 13 and 14 contain the comparable HSFR results for no flow and through flow, respectively. In comparing the standing waves for both flow conditions, the HSFR program describes the standing waves in the system very well. Detailed numerical comparison of the wave shape versus length results is made difficult by the lack of numerical data for the Hillman results. The HSFR results are plotted as a cubic spline through the analysis results at the junctions of the line elements in the HSFR model (Fig 6). For the no flow condition, HSFR predicted standing waves at 2.1, 17.1, and 25.8 Hz which compare well with the reported test data of 2.1, 16.5, and 25.0 Hz (Ref 11:192). These HSFR results differ from the test data by 0.%, 3.6%, and 3.2%, respectively and are within 1 Hz of the test data for all modes. For the through flow condition, HSFR predicted standing waves at 2.7, 19.2, and 25.8 Hz, compared to the test data at 2.1, 18.7, and 25.0 Hz, respectively. For comparison the HSFR impedance results for the through flow condition were 2.1, 19.2, and 25.8 Hz, respectively. The percent differences for the HSFR standing wave frequencies and the test data were 28.6%, 2.7%, and 3.2%, respectively, and are also within 1 Hz for all modes. The difference between the impedance results and the standing wave results within HSFR for the first mode are due to the fact that the impedance results represent conditions at the pump inlet location and the standing wave plot represents the entire line length. The standing wave plots were defined by the frequency of the greatest pressure amplitude throughout the system, and a bandwidth of .75 Hz (5 rpm) was specified to distinquish
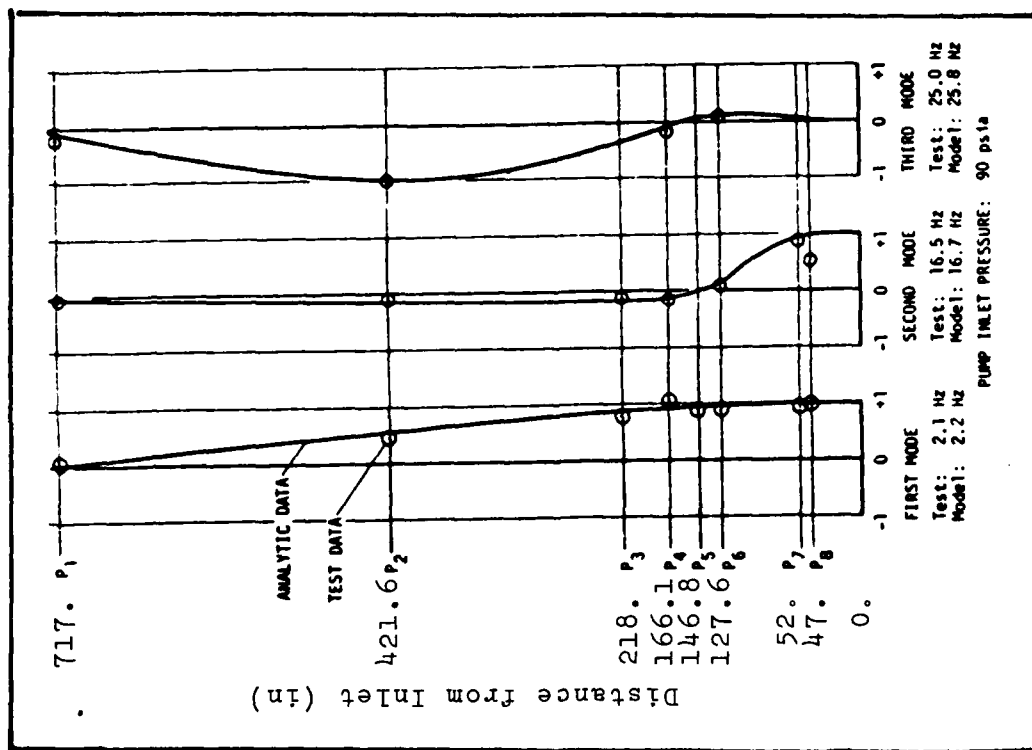
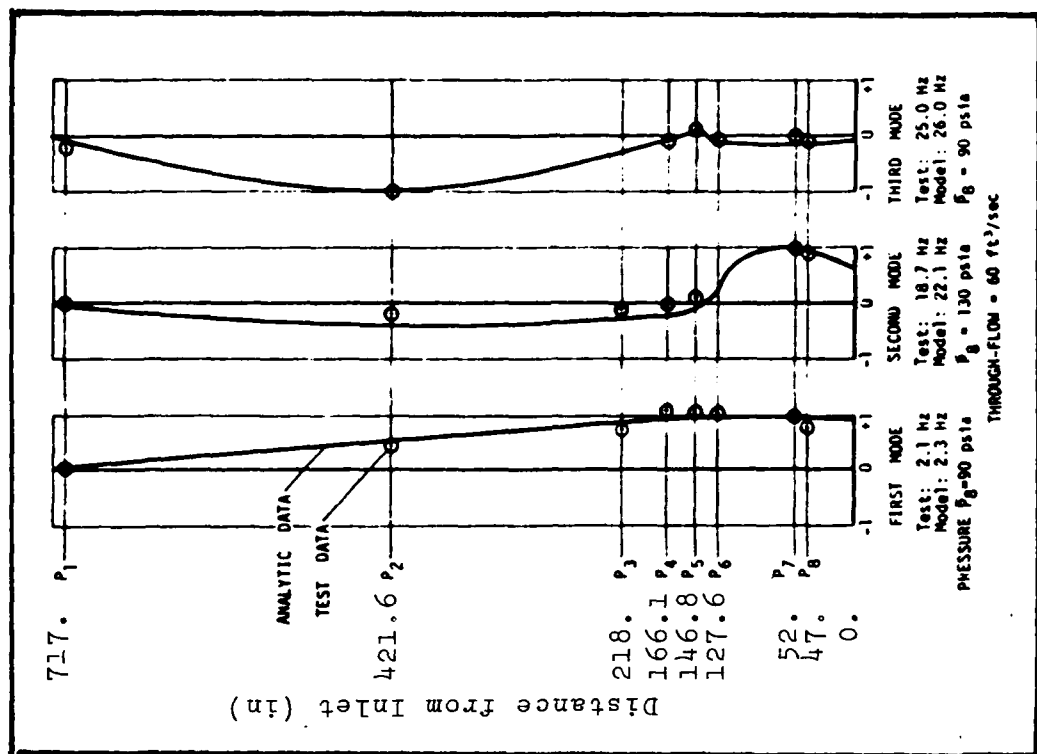33

Fig 12. Hillman's Normalized Pressure Wave Shapes for 60cfs Through Flow (Ref 11: 192)
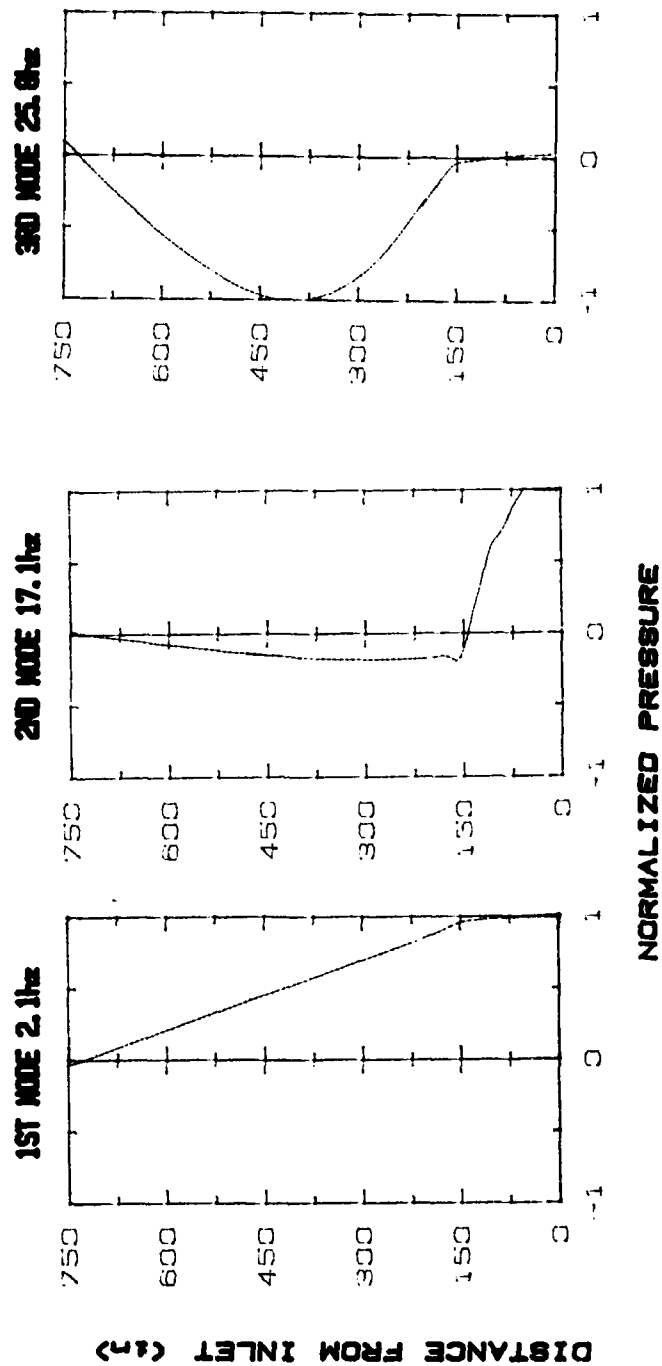
Fig 11. Hillman's Normalized Pressure Wave Shapes for No Flow (Ref 11: 192)

34

Fig 13. HFSR Normalized Pressure Wave Shapes for No Flow
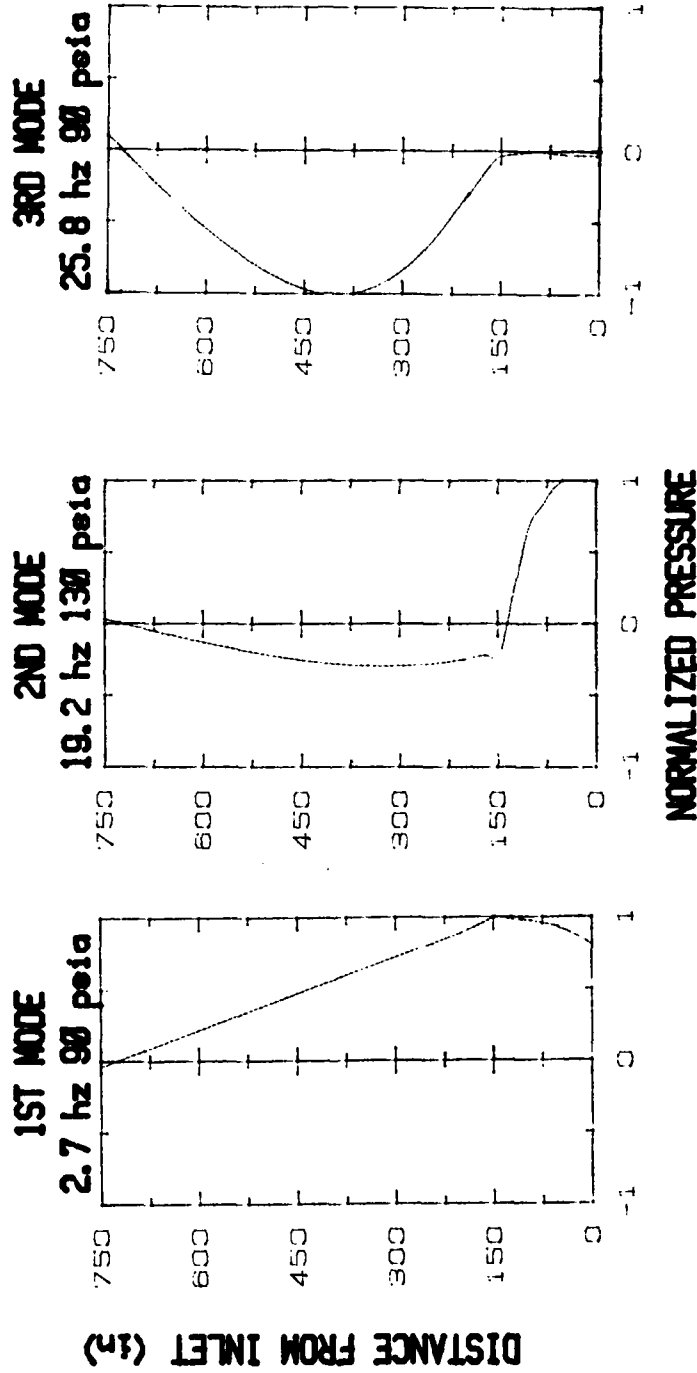
35

Fig 14. HFSR Normalized Pressure Wave Shapes for 60cfs Through Flow

separate standing waves. Thus the predicted standing wave at 2.7 Hz overrode any standing wave which might have been plotted for 2.1 Hz. Table VII summarizes all the measured standing wave frequencies reported by Hillman together with the analytical results reported by Hillman and the HSFR standing wave and impedance frequency results.

Table VII

Comparison of Analytical Frequency Results

| | | STANDING WAVE | | | | IMPEDANCE | |
| | TEST | HILLMAN'S | | HSFR | | HSFR | |
MODE	DATA	FREQ	% DIFF	FREQ	% DIFF	FREQ	% DIFF
NO-FLOW							
FIRST	2.1	2.2	4.8	2.1	0.	2.1	0.
SECOND	16.5	16.7	1.2	17.1	3.6	17.1	3.6
THIRD	25.0	25.8	3.2	25.8	3.2	25.8	3.2
THROUGH-FLOW							
FIRST	2.1	2.3	9.5	2.7	28.6	2.1	0.
SECOND	18.7	22.1	18.2	19.2	2.7	19.2	2.7
THIRD	25.0	26.0	4.0	25.8	3.2	25.8	3.2

Sensitivity Study Results

The sensitivity study compared the HSFR analytical results with the Boeing test data previously published by Brod (Ref 13). These test data were reported as plotted bands of measured data for each frequency mode in each sensitivity study. For comparison with the HSFR results these plotted test results were digitized from the Brod report using an Hewlett Packard HP 85A microcomputer with a HP Model 7225B digitizing plotter and then replotted with the HSFR results, which are the predicted impedance resonant frequencies from separate computer runs for each analysis condition. In the HSFR analyses, all the element input data were held constant except for those data directly associated with the parameter under investigation. While this procedure provided insight into the sensitivity of HSFR to changes in the input data, it may have caused difficulties in the comparison with the test data, as aspects of the physical system were not realistically modeled in the HSFR analyses throughout the entire range of the sensitivity comparisons.

The effect of the gas volume in the prevalve accumulator is presented in Fig 15. Boeing data and HSFR results are plotted for the first and second frequency modes, at pump inlet pressures of 58 and 130 psia (Ref 13:51). The HSFR results for the first frequency mode track well with the test data band. The second frequency mode results at 130 psia are within the test data band between the 60 and 100% gas volumes, but are higher than the test data for volumes below 50%. The 58 psia, second mode results are uncharacteristically higher that the test data throughout the range of gas volumes. These discrepancies will be discussed later.

The sensitivity of the gas volume in the cavitation accumulator was investigated using first mode test data at 110 psia pump inlet pressure (Ref 13:37), and the results are plotted in Fig 16. The HSFR results are within the band of test data at 0% and 50% gas volume, but are higher than the test data between those two conditions. This slight difference is not considered significant and is attributed to inaccuracies in
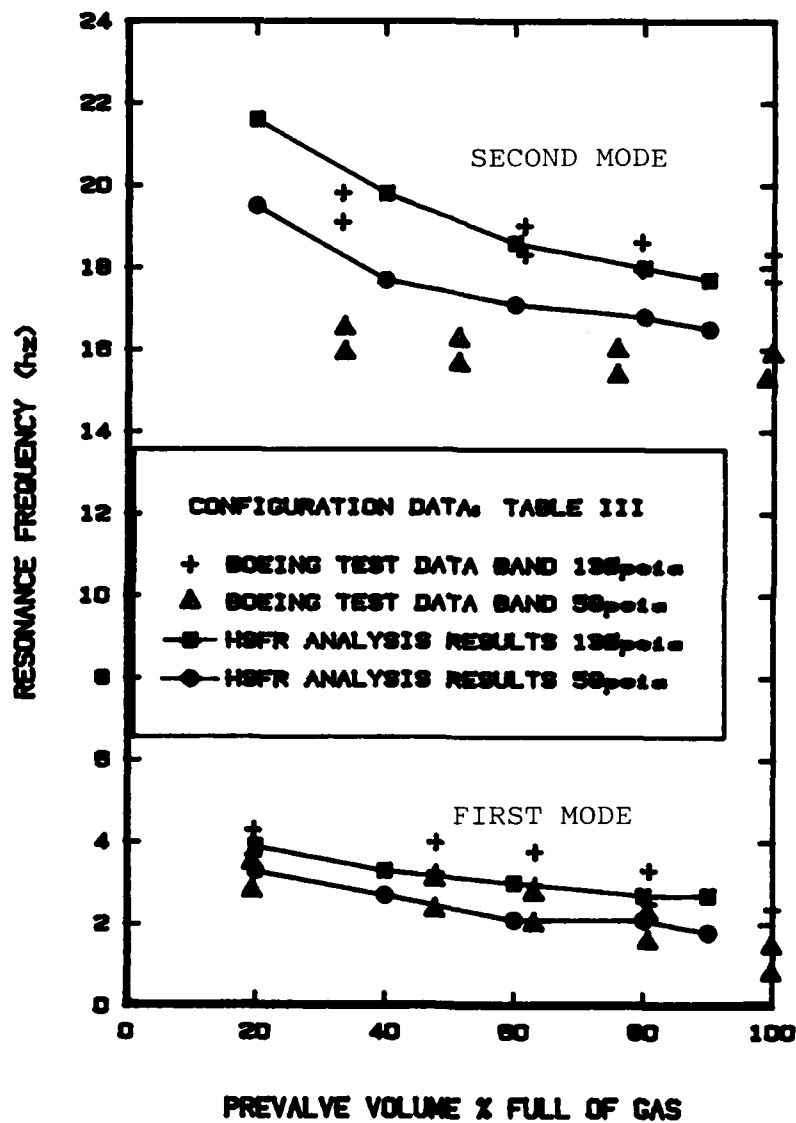
38

Fig 15. Prevalve Accumulator Sensitivity Results

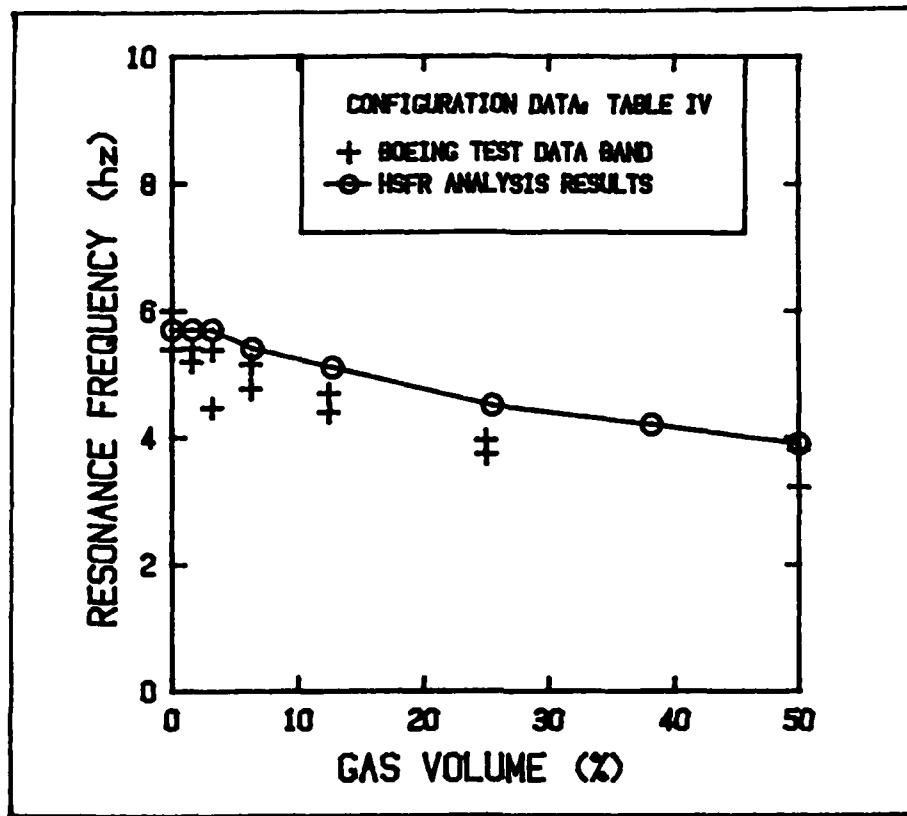representing the accumulator in the HSFR model.

Fig 16. Cavitation Accumulator Sensitivity Results

Two different system configurations were used to investigate the pump inlet pressure sensitivity. The first configuration results (Fig 17) show that HSFR is unaffected by changes in the pump inlet pressure when the feed system does not include the cavitation accumulator and there is no gas pressure in the prevalve accumulator (Table V) (Ref 13:14). The test data does show a sensitivity to the inlet pressure in the first mode response, but not in the second mode (Ref 13:40). In the second configuration, described in Table VI, both the test data (Ref 13:47) and the HSFR results show much more sensitivity the inlet pressure (Fig 18). This configuration includes the gas pressure inside the prevalve accumulator, and third mode test data are reported. This plot shows a discrepancy between the HSFR results
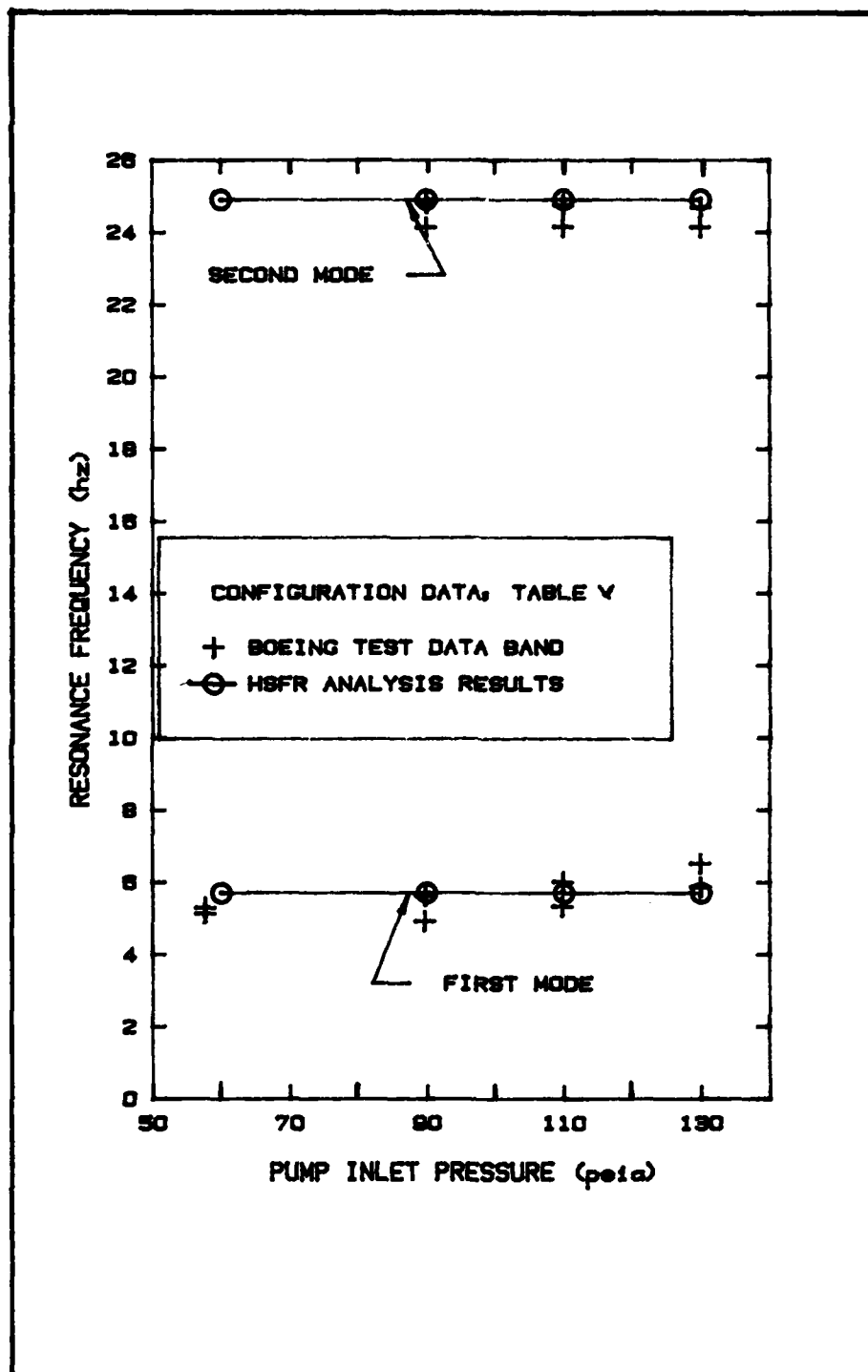
40

Fig 17. Pump Inlet Pressure Sensitivity
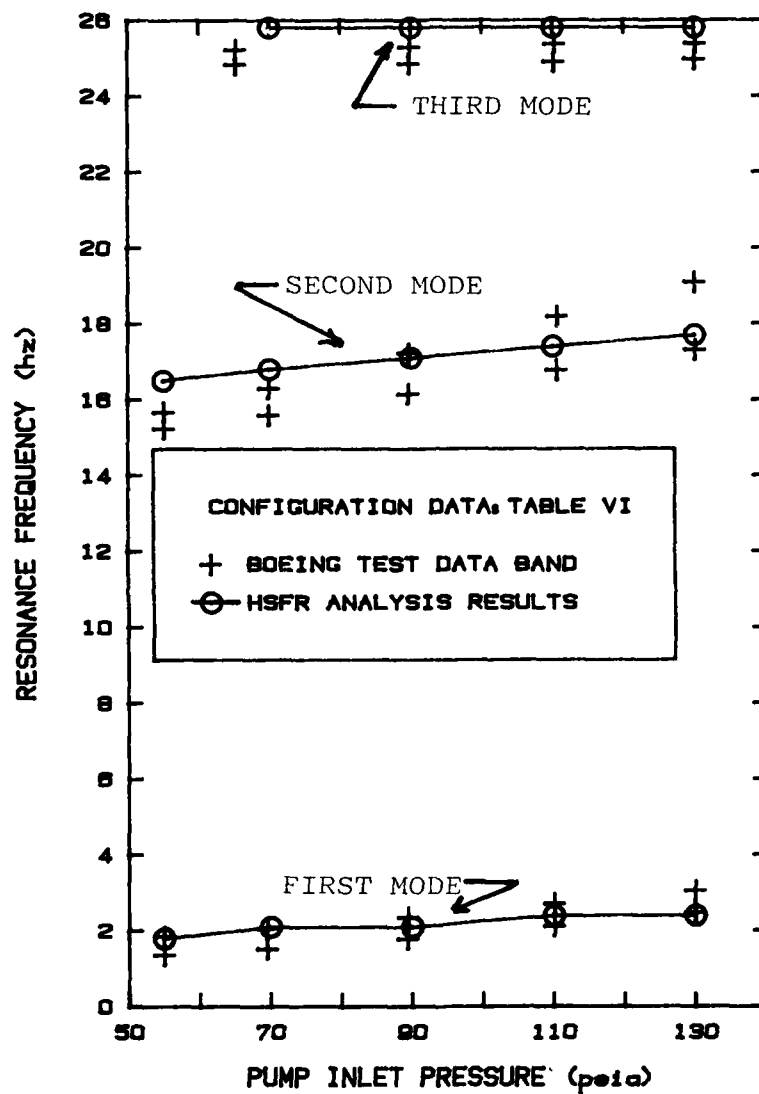Results Without Prevalve Accumulator

41

Fig 18. Pump Inlet Pressure Sensitivity
Results With Prevalve Accumulator

42

and the Boeing test data in the second mode results. This will be discussed later.

The final sensitivity study investigated the effect of the steady state temperature of the HSFR results (Fig 19). No test data were available for comparison to the HSFR results, but previous investigations with HSFR, which used hydraulic oil as the working fluid, showed a strong temperature sensitivity within HSFR (Refs 7:65 and 14:111). The analyses done in this investigation with water as the test fluid show no sensitivity to temperature in the range of interest. This significant difference from what was previously known about HSFR will be discussed in the next section.

One of the disadvantages of other analysis programs discussed in Section I was the long execution time, which affects the operating cost and turnaround time. For the analyses done in this investigation, HSFR required 75 seconds of central processor time on a CDC Cyber 170/730 and had core memory requirements of 52000, which is not excessive.

Discussion of Discrepancies

In the comparison with the Hillman results, the HSFR phase angle results were opposite in sign from Hillman's (Figs 8-10). The HSFR phase angle was defined as the flow phase angle minus the pressure phase ngle, based on information provided by Hillman (Ref 20). This definition was opposite of one used in HSFR to compute the energy density (Ref 10: Sec 2,26) but Hillman's definition was used for comparison with his results. Since the HSFR results are opposite in sign from Hillman's, it is assumed that the definition provided over the phone in Ref 20 was backwards. There was over ten years of lapsed time between Ref 11 and Ref 20.

The sensitivity studies which had significant discrepancies between the HSFR results and the Boeing test data were: the effect of the prevalve accumulator (Table III and Fig 15); and the effect of pump inlet pressure (Tables V and VI and Figs 17 and 18); and the lack of temperature sensitivity (Fig 19).
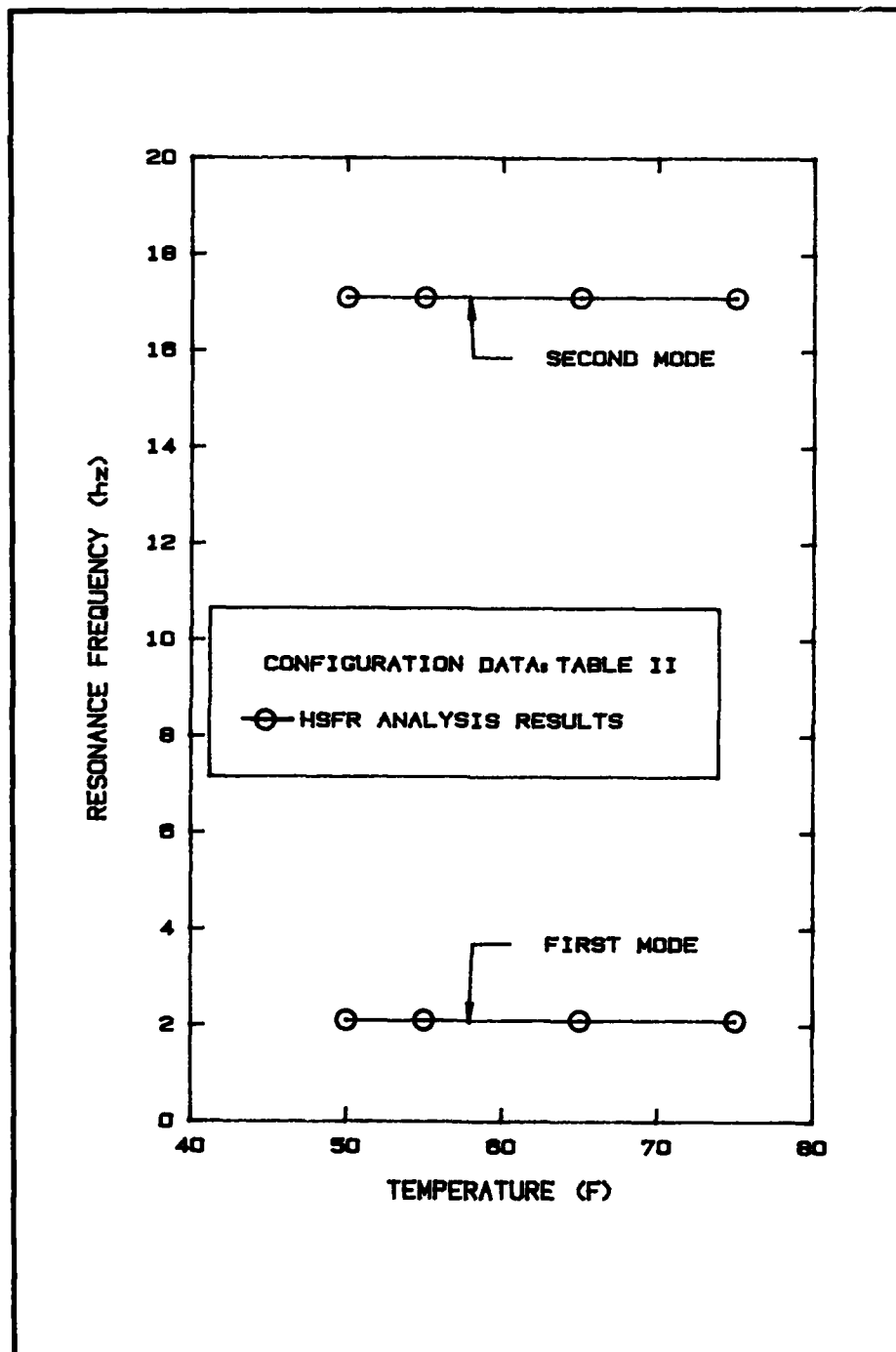
43

Fig 19. Temperature Sensitivity Results

As mentioned earlier, the sensitivity studies were analyzed with all the input data being held constant except for those values directly associated with the parameter being investigated. In identifying the cause of the discrepancies, attention was focused on what hidden variables existed because of this analysis procedure. These hidden variables were probably overriding the sensitivity of the parameter under investigation and causing the HSFR results to differ from the test data. The hypothesis that the discrepancies are related to the input data and not to the HSFR model gains validity from the previously discussed agreement between the HSFR results and the Hillman comparisons (Table VII).

In order to identify the hidden variables causing the second mode discrepancy seen in Fig 15 which was the effect of the prevalve accumulator gas volume, it was necessary to study all the relevant sensitivity studies. In all three comparisons (Figs 15, 17, 18), the Boeing test data were reported for a range of pump inlet pressures, and the HSFR analyses were done with the component under investigation at the correct pressure. However, as discussed earlier, the pressure sensitive components in the system which were not under investigation were modeled using 90 psia data (Table I). In the effect of prevalve gas volume study (Fig 15), the pump cavitation accumulator (Elements 13, 14, 15 in Fig 6) and the acoustic wavespeeds within the pressure-volume compensator (PVC) duct (Elements 17, 18, 19 in Fig 6) were modeled at the 90 psia values for both the 58 and 130 psia conditions. The pump inlet pressure sensitivity results shown in Fig 17 do not include the cavitation accumulator or the prevalve accumulator in the model, while the results shown in Fig 18 include both the cavitation accumulator, modeled at 90 psia, and the prevalve accumulator modeled at the pump inlet pressure reflected in the data (Tables V and VI). Thus the only common hidden variable in these three separate sets of analyses is the wavespeed of the PVC duct, which was held constant at the 90 psia values reported by Hillman (Ref 11:190). Studying the three sets of results simultaniously, the HSFR results agree the best with

45

the Boeing test data at the 90 psia inlet pressure condition, and tend to be higher than the test data at lower inlet pressures and lower then the data at higher pressures. This can be seen most clearly in the second mode results in Fig 18. Thus the three pressure related discrepancies are related to the PVC duct acoustic wavespeed data.

The final discrepancy addressed is the lack of sensitivity to temperature changes demonstrated by HSFR during this investigation (Fig 19). A study of the HSFR program shows that the only use of the steady state temperature is by the FLUID subroutine for calculating the three fluid properties used in the mathematical models. Previous investigations of the HSFR program (Refs 7, 8, 14-16) used hydraulic oils as the working fluid, and Mil-H-5606B hydraulic oil was used in the AFIT studies (Refs 14-16). This difference in working fluid prompted a comparison of the fluid properties as a possible explanation of the different temperature sensitivities. The kinematic viscosity and bulk modulus values of water and Mil-H-5606B hydraulic oil are plotted versus temperature in Fig 20. This comparison shows the kinematic viscosity of the hydraulic oil is an order of magnitude higher than that of water, yet the relative change of the property per change in temperature is the same as shown by the similar slopes of the lines. The change in bulk modulus per change in temperature between the two fluids are not the same, however, even though the bulk modulus values are of the same magnitude. The density values are not shown because there is not any appreciable difference in density between the two fluids. The predominate use of the fluid properties within HSFR is in the LINE subroutine. The bulk modulus is used to compute the acoustic wavespeed for the fluid and the duct wall, and the kinematic viscosity is used to compute the frequency dependent friction factor. Since the acoustic wavespeed calculation was not used in this investigation, the order of magnitude difference in the kinematic viscosity is identified as the cause of the change in temperature sensitivity.
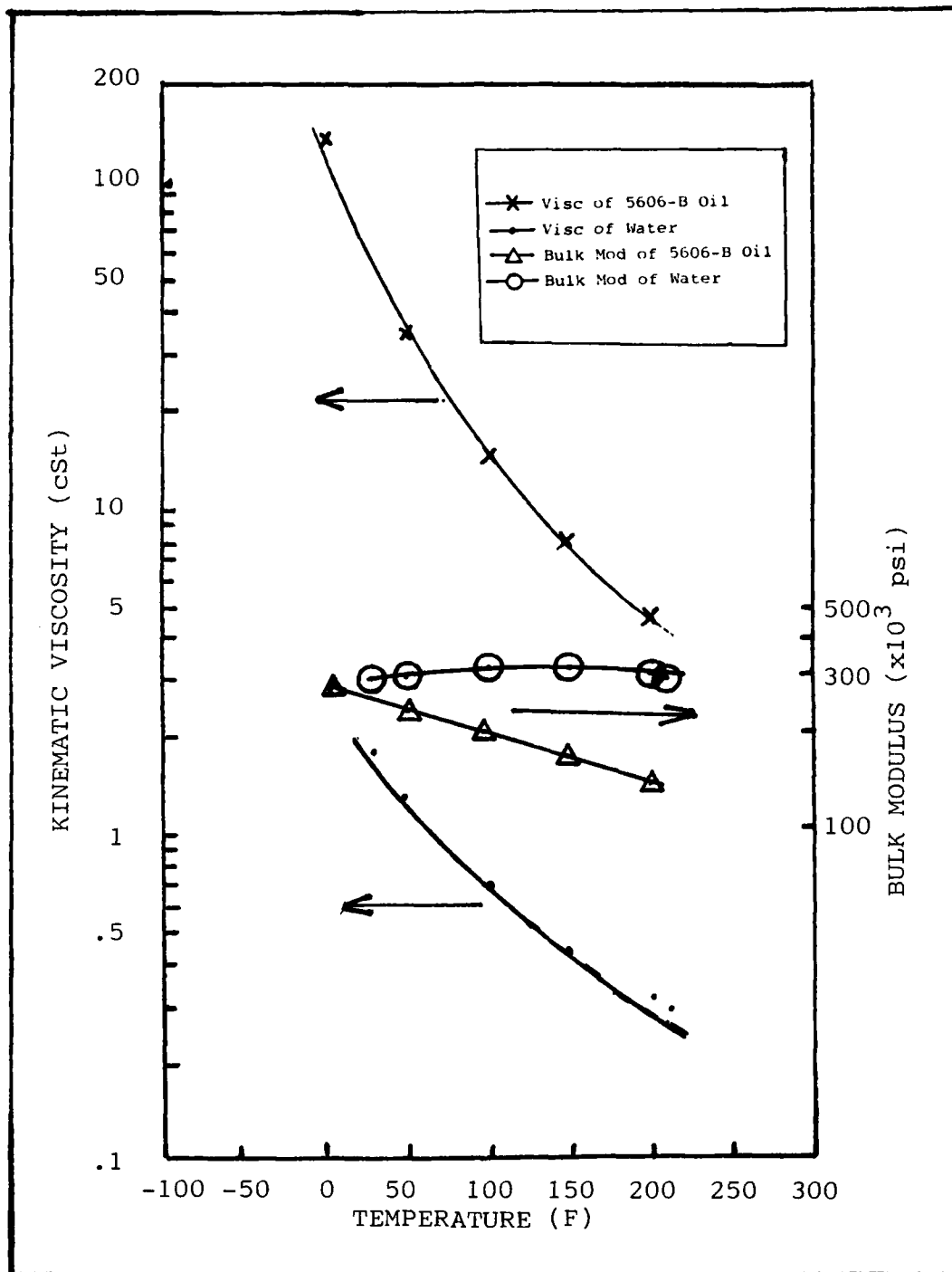
Fig 20. Comparison of Fluid Property Values

V. Conclusions

The objective of this investigation was to determine the applicability of the HSFR program in conducting a frequency response analysis of a liquid propellant feed system. This objective was approached by analyzing an experimental propellant feed system and comparing the HSFR results with two sets of previously published data, Hillman (Ref 11) and Brod (Ref 13). With this effort completed, the following general and specific conclusions are made.

In terms of the objective of this investigation, the HSFR program is applicable to the analysis of current pump fed propellant feed systems. The agreement of the HSFR results with the test data clearly demonstrated this. Overall, HSFR had lower percent differences than the linearized impedance model used by Hillman (Ref 11) as was shown in Table VII. However, HSFR is not ready for use by the system design analyst because the level of confidence in the HSFR results is low. In order to improve this level of confidence to that which HSFR has for hydraulic systems, more comparisons must be made with other experimental systems. Several times during this investigation, the propellant system was modeled in an acceptable yet improper way and comparison with the test data was the only way the modeling error was detected. Recommendations for further work which will address this level of confidence are made in the next section.

Some specific conclusions about the programming approach of HSFR, the program structure and analytical results can be made, based of the lessons learned during this investigation and the results of the analyses.

From a programming viewpoint, the ease with which modifications were made to the HSFR program demonstrate the flexibility and adaptability of the program structure. Because of this design structure, new algorithms were easily incorporated into existing subroutines, and entire subroutines were replaced with little difficulty.

Changes in the output format and extraction of additional results from the program were also easily accomplished, as was demonstrated by the pressure gain plotting option which was developed during this investigation.

From an analytical viewpoint, several additional conclusions can be made from the results of this investigation. The first analytical conclusion is that the use of a acoustic source in the HSFR model different from that used in the experimental system does not affect the frequency response analysis of the system. This conclusion is based on the agreement between the test data generated with a pulsating valve and the HSFR results which used a nine piston pump model.

The second conclusion from the analytical phase of this investigation relates to the sensitivity study results. These sensitivity comparisons indicated that the mathematical models in the HSFR program are sensitive to: the working fluids kinematic viscosity; the acoustic wavespeed corrected for the elasticity of the wall material; and the compliance of the volume elements, for both gas filled and water filled volumes.

VI. Recommendations

While the overall conclusion of this investigation is that HSFR is fundamentally applicable to the analysis of liquid propellant feed systems, several recommendations for the directions of future work are possible. These recommendations are based on difficulties encountered during this investigation and on the directions the liquid rocket community is going with feed system technology.

Difficulties were encounted in accurately modeling the experimental feed system for analysis with HSFR. In order to eliminate these difficulties and make HSFR useful to the feed system designer, well characterized models of generalized feed system components need to be developed. This effort, which would be similar to the original McDonnell Aircraft Company project, would eliminate much of the trial and error procedure in modeling pump inducers, visor valves, flexible line segments, pressurized tanks and pressurized cavities. Many unsuccessful analyses were done during this investigation because there were insufficient physical parameters available to describe the propellant components with the existing HSFR component models. Development of liquid rocket component models would resolve this.

Future directions in feed system designs are pointing toward very short vehicles with toroidal tanks. While some designs under development involve some large length to diameter ratios, such as an improved Atlas type vehicle and new expendable launch vehicles, most of the government efforts are focusing on Shuttle compatable orbital transfer vehicles. The analysis issues involved with these designs are much more complex than the resonant frequency analyses accomplished by HSFR. A significant issue in current feed system development effort is the three dimensional fluid dynamics of the propellant in the tank in a orbital environment.

Because of the requirement for uniform flow patterns within the toroidal feed systems during orbital operations, feed system analysts are now using the hydroelastic

models within NASTRAN, and other advances in computational fluid dynamics.

Even with these three dimensional fluid dynamic problems existing in current feed system designs, the liquid rocket community is still using the computer program used by Hillman in his work with the Saturn S-IC LOX suction duct for preliminary frequency response studies (Ref 21). Further development of HSFR, in the form of the work recomended here, would provide the community with an alternate frequency response program which is easy to use and inexpensive to operate.

BIBLIOGRAPHY

1.   Liquid Propellant Rocket Combustion Instability, NASA SP-194. David T. Harrje, ed. Washington D.C.: Scientific and Technical Office, National Aeronautics and Space Administration, 1972.

2.   Holster, J. L. and J. Astleford. "Analytical Model for Liquid Propellant Feedline Dynamics", Journal of Spacecraft and Rockets, II: pp 180-187 (March 1974).

3.   Holster, J. L., J. Astleford and C. R. Gerlach. Analysis of Propellant Feedline Dynamics, Final Report NASA CR-124308.   Southwest Research Institute, San Antonio, Texas. May 1973.

4.   D'Souza, A. F. and R. Oldenburger. "Dynamic Response of Fluid Lines", Journal of Basic Engineering, Trans ASME, 87: pp 589-598, (September 1964).

5.   Rubin, Sheldon. "Longitudinal Instability of Liquid Rockets Due to Propulsion Feedback (POGO)", Journal of Spacecraft and Rockets, 3: pp 1188-1195 (August 1966).

6.   Webber, W. T., E. Y. C. Wong and M. Toniguichi.   Transient Performance Program, Vol II, User's Manual. Final Report, 1 Oct 1977 to 31 Oct 1980, AFRPL-TR-80-22, Edwards AFB, CA: Air Force Rocket Propulsion Laboratory, January 1981.

7.   Amies, Gerry, J. B. Greene, R. J. Levek and N. J. Pierce. Aircraft Hydraulic Systems Dynamic Analysis: Final Report AFAPL-TR-77-63. Wright-Patterson AFB, Ohio: Air Force Aero Propulsion Laboratory, October 1977.

8.   DeGarcia, H., J. B. Greene, R. J. Levek and N. J. Pierce. Aircraft Hydraulic Systems Dynamic Analysis: Final Report, February 1977-September 1978 AFAPL-TR-78-77. Wright-Patterson AFB, Ohio: Air Force Aero Propulsion Laboratory. October 1978.

9.   Amies, Gerry and Bob Green. Aircraft Hydraulic Systems Dynamic Analysis Vol III - Frequency Response (HSFR) Computer Program User Manual: Interim Technical Report, AFAPL-TR-76-43 Vol III.   Wright-Patterson AFB, Ohio: Air Force Aero Propulsion Laboratory. February 1977.

10.----. Aircraft Hydraulic Systems Dynamic Analysis Vol IV - Frequency Response (HSFR) Computer Program Technical Description: Interim Technical Report, AFAPL-TR-76-43 Vol IV. Wright-Patterson AFB, Ohio: Air Force Aero Propulsion Laboratory. February 1977.

11. Hillman, H. F., B. F. Kerkam and G. D. Poel. "Application of Linearized Friction Impedance Models to Complex Fluid Systems.", Journal of Fluids Engineering, Trans ASME, 95: pp 189-196 (June 1973).

12. Rohmann, C. P and E.C. Grogan. "On the Dynamics of Pneumatic Transmission Lines". Transactions of the ASME, 79: pp 853-874 (May 1957)

13. Brod, E. J., J. C. Angehr and R. L. Rich. LOX Suction Duct Dynamic Evaluation, D13339, Summary of Test Results. The Boeing Company Report D5-14061, May 1970.

14. Wright, John A. An Experimental Study of Hydraulic System Frequency Response Characteristics. Unpublished Thesis. Wright-Patterson AFB, Ohio: Air Force Institute of Technology. 1977.

15. Katz, S. An Experimental Study of Measuring Oscillatory and Transient Pressure in Hydraulic Systems. Unpublished thesis. Wright-Patterson AFB, Ohio: Air Force Institute of Technology. 1978.

16. Pletcher, John A. An Analytical and Experimental Study of Aircraft Hydraulic Lines Including the Effect of Mean Flow. Unpublished PhD Dissertation, Wright-Patterson AFB, Ohio: Air Force Institute of Technology. 1979.

17. Handbook of Mathematical Functions with Formulas, Graphs, and Mathematical Tables. Seventh Printing. Milton Abramowitz and Irene Stegun, eds. National Bureau of Standards Applied Mathematics Series 55. US Dept of Commerce. May 1968.

18. 1980 IR&D Program, Boeing Commercial Airplane Company. The Boeing Company. pp 5-221, 5-226 - 5-228.

19. Trikha, A.K. "An Efficient Method for Simulating Frequency Dependant friction in Transient Liquid Flow." Journal of Fluids Engineering, Trans ASME, 97: pp 97-105 (March 1975)

20. Hillman H.F. Boeing Military Aircraft Company. Telephone conversation, Seattle, Washington. 2 December 1982.

21. Advanced Spacecraft Feed Systems, Vol I, Technical Proposal: Report MDCE2509. McDonnell Douglas Astronautics Co. St. Louis, Missouri. 30 April 1982.

22. AFRPL-TDR-64-25 Aerospace Fluid Component Designer's Handbook. Vol. II, Chapter 12. Edwards AFB, California: Air Force Rocket Propulsion Laboratory, February 1970.

23. Daugherty, Robert L. and Joseph B. Franzini. Fluid Mechanics with Engineering Applications (Seventh Edition). New York: McGraw - Hill Book Company, 1977. p. 539

24. AFML-TR-67-107. Fluids, Lubricants, Fuels, and Related Materials, Part 1 Technical Report: Wright-Patterson AFB, Ohio: Air Force Materials Laboratory, March 1967. pp 13-80.

25. Meyer, C.A.,R. B. McClintock, G. J. Silvestri and R. C. Spencer. Thermodynamic and Transport Properties of Steam. New York: American Society of Mechanical Engineers, 1967. p. 295.

26. Handbook of Fluid Dynamics. Victor L. Streeter, ed. (First Edition). New York: McGraw - Hill Book Company, 1961. Section 1, 4.

27. Kreysig, Erwin. Advanced Engineering Mathamatics (Third Edition). New York: John Wiley and Sons, 1972. p. 479.

APPENDIX A

HYDRAULIC SYSTEM FREQUENCY RESPONSE (HSFR)

PROGRAM USER'S MANUAL

Appendix A

Hydraulic System Frequency Response (HSFR)

Program User's Manual

This appendix describes the operating procedure for the Hydraulic System Frequency Response (HSFR) program, where that procedure differs from the instructions provided in the HSFR User's Manual (Ref 9). Not intended as a complete manual, this information serves as a supplement to the HSFR User's Manual. This Appendix is arranged in sections which follow the order of the program input data, with references to the applicable pages of the HSFR manual where possible.

The program input deck is divided into three sections; first, the general system description; second, the cards which describe the individual components in the system; and third, the cards which specify the output plots desired. Within the first and third sections, the input cards have a specific order which must be followed (Ref 9: Sec 2, 7 - 13 and 52 - 57). The component cards in the second section must be in the order of the system being described, beginning with the pump (Ref 9: Sec 2, 1 - 7).

Card 2-Number of Elements, Fluid, Temperature, and Pressure (Ref 19: Section 2, 9-11)

In HSFR, Card 2 contains the same type of information as for the original HSFR, except the types of fluids are different and the inlet system pressure may be specified. The four fluids and their respective codes are shown in Table VIII, which replaces the one for Card 2 in the HSFR manual (Ref 9: Sec 2, 10). The option for the user to input the density, adiabatic bulk modulus and kinematic viscosity data directly still exists, however, if it is used, an additional card must be added with the fluid title on it. This card comes immediately after Card 3, Pump Speed and Frequency Data.

Table VIII

Card 2 Information

COLUMNS	FORMAT	DATA	DIMENSIONS
1-5	I5	Total number of circuit elements	
10	I1	Fluid type: user option = 0 or 6	
		MMH = 1	
		RP-1 = 2	
		N_2O_4 = 3	
		Water = 4	
11-20	F10.0	System Temperature	$^\circ$F
21-30	F10.0	System Pressure	psig
31-40	F10.0	Fluid viscosity or blank	in^2/sec
41-50	F10.0	Fluid density or blank	$lb\text{-}sec^2/in^4$
51-60	F10.0	Fluid adiabatic bulk modulus or blank	psi
61-70	F10.0	System Inlet Pressure	psig

Card 3 Pump Speed and Frequency Data

The change in the Card 3 information deals with the standing wave plotting feature (Ref 9: Sec 2, 12-13). This capability was added to the HSFR program after the manuals were published, and an additional change was made in this investigation. These instructions apply to this HSFR version only. Standing wave plots can be requested for any section of line where the peak pressure exceeds a specified value or at any specified pump speed, or for both conditions. Depending on which standing wave plot options are desired, between one and three additional data cards will be necessary, which are placed at the end of the third section in the data deck. A maximum of ten plots can be made in each catagory; Resonant Test Pressure or Selective Pump Speed. A logic chart (Fig 21) has been devised to determine what information is necessary for the standing wave plot capability.
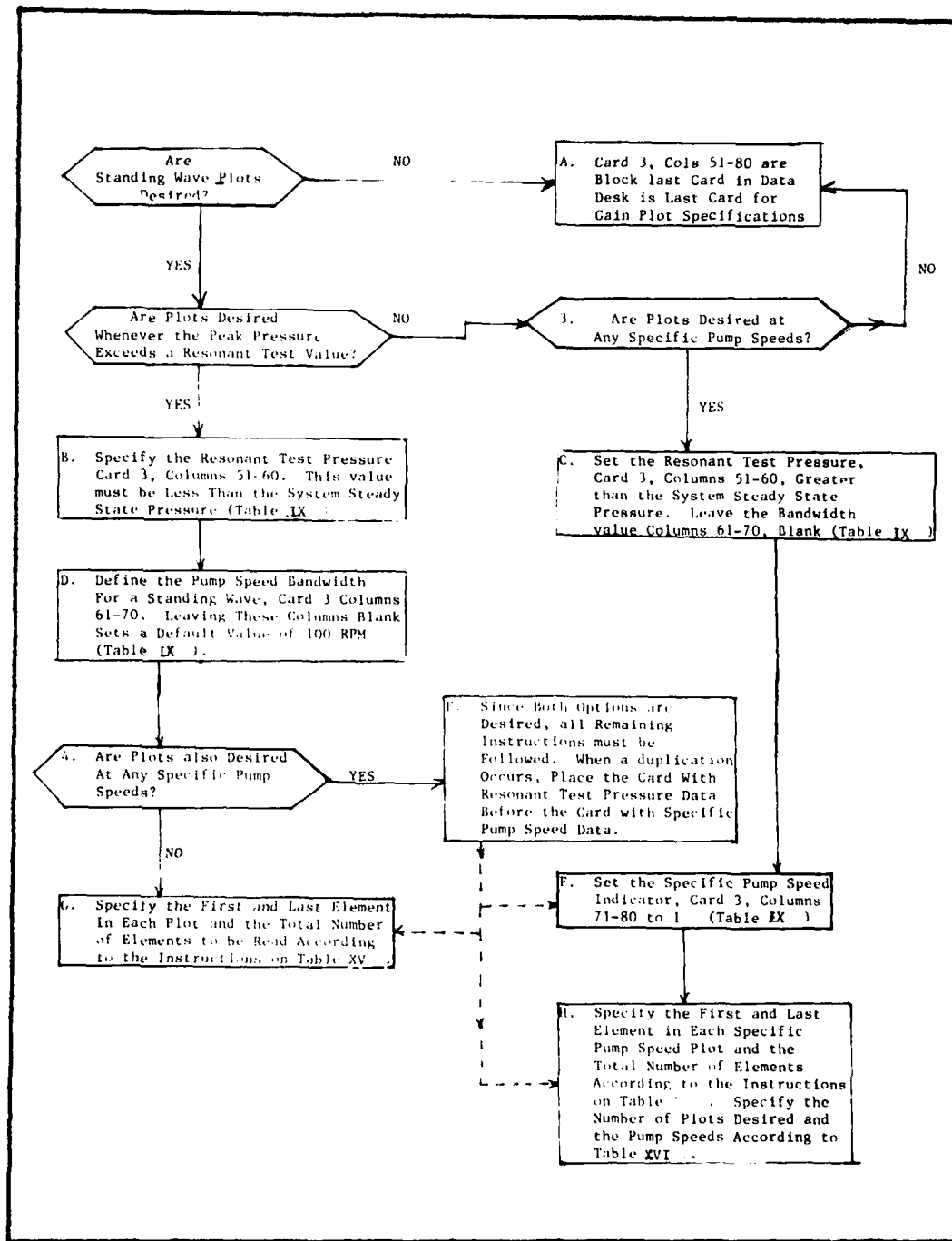
Fig 21.

Logic Diagram for Standing Wave Plots

Table IX

Card 3 Information

COLUMNS	FORMAT	DATA	DIMENSIONS
1-10	F10.0	Start Speed	rpm
11-20	F10.0	Finish Speed	rpm
21-30	F10.0	Speed Increment	rpm
31-40	F10.0	First Harmonic = 1., 0, or blank	
		Second Harmonic = 2.	
		Third Harmonic = 3.	
		etc. =10. maximum	
41-50	F10.0	Number of pumping pistons	
51-60	F10.0	Standing Wave Resonant Test Pressure	psi
61-70	F10.0	Standing Wave Band Width	rpm
		Default value of 100 rpm set by leaving blank	
71-80	F10.0	Selective Pump Speed	
		No = 0, or blank	
		Yes = 1.	

Card 3A User Specified Fluid Name

This card is only used if the fluid properties were specified on Card 2. If the program's internal fluid property calculations are used, then this card is to be left out of the input completely.

The only information in this card is the fluid name, such as "liquid oxygen".

Table X

Card 3A Information

COLUMNS	FORMAT	DATA	DIMENSIONS
1-24	3A8	Fluid name	

Line Element Input Data

The input data required for rigid lines or tubing are shown below (Ref 9: Sec 2,15-16). The user now has the option of allowing the program to compute the acoustic wavespeed for the fluid filled element or supplying the value directly. If the wavespeed is supplied, the outside diameter, wall thickness and modulus of elasticity data are not needed. Instead, the inside diameter and wavespeed should be provided as shown. A discussion of the internal wavespeed equation is provided in the HSFR Program Technical Manual (Ref 10: Sec 5, 1-2).

Table XI

Line Element Data Card

COLUMNS	FORMAT	DATA	DIMENSIONS
1-5	I5	NTYPE = 1	
10	I1	KTYPE = 0 or blank	
11-20	F10.0	Line length	in
21-30	F10.0	Line diameter - outside or inside	in
31-40	F10.0	Wall thickness or blank	in
41-50	F10.0	Modulus of elasticity or blank	psi
51-60	F10.0	Blank or acoustic velocity	in/sec

61

Volume Element Input Data

The input data for volume elements or lumped compliance are shown below. This data will only work with the volume subroutine version developed during this investigation. Liquid filled volumes (KTYPE = 0) are treated in the original version of the subroutine, which is discussed in the HSFR User's Manual (Ref 9: Sec 2, 24-25)

TABLE XII

Volume Element Data Card

Columns	Format	Data		Dimensions
1-5	I5	NTYPE = 3		
6-10	I5	KTYPE	0 or Blank = Liquid filled	
			1 = Gas filled	
			2 = Direct Input Compliance	
For KTYPE = 0 the following datum is required				
11-20	F10.0	Volume		in^3
For KTYPE = 1 the following data is required				
11-20	F10.0	Volume		in^3
21-30	F10.0	Steady State Pressure of Gas		psia
31-40	F10.0	Ratio of Specific Heat for Gas		-
For KTYPE = 2 the following datum is required				
11-20	F10.0	Compliance		psi/cis

Phase Angle and Gain Plot Capabilities

Input data cards are required to specify the desired program output plots. Seven variables are available for plotting and must be requested in the following order: flow, pressure, impedance, acoustic energy density, acoustic intensity, phase angle between the flow and pressure, and the pressure gain. At least one card is required in each catagory, and if no plots are desired then a blank card must be included in the proper sequence. The program will not operate properly if there are not at least seven cards following the last system element description card. The standing pressure wave plots are requested in a different manner and blank cards are not required if standing pressure waves are not plotted.

The format for the first six variables; flow, pressure, impedance, acoustic energy density, acoustic intensity and phase angle, is the same for each case and is shown in Table XIII. While the original HSFR program plotted the impedance in decibles, this was changed to the complex absolute value during this investigation. The phase angle plotted is the difference between the phase angles of the complex flow and complex pressure (Fig 22).
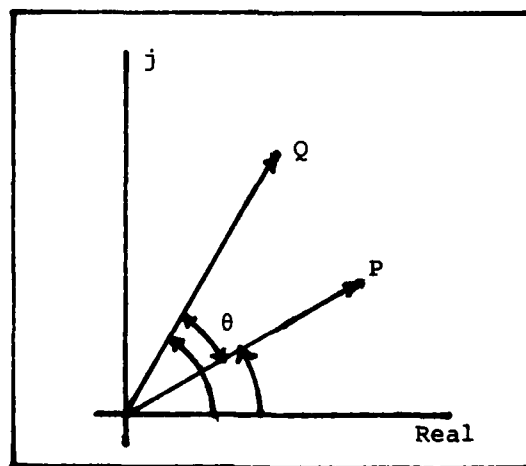

Fig 22. Phase Angle Definition

Table XIII

First Set of Output Data

(Six of these cards are required, blank cards indicate no plots desired)

COLUMNS	FORMAT	DATA	DIMENSIONS
1-5	I5	Number of plots for one category	-
6-10	I5	Element number for first plot	-
11-15	I5	Element number for second plot	
16-20	I5		
21-25	I5		
26-30	I5		
31-35	I5		
36-40	I5		
41-45	I5		
45-50	I5		
51-55	I5		
56-60	I5		
61-65	I5		
66-70	I5		
71-75	I5		
76-80	I5	Element number for fifteenth plot	

Pressure gain plots are requested by specifying the total number of elements to be read, followed by the sending element and receiving element used in each plot. Since two elements are required for each plot, the number of elements specified is twice the number of plots desired (Table XIV). A maximum of ten plots, or twenty elements, can be specified. As with the first six output variables, the program will continue reading element numbers on a second card, until the specified number of elements have been read. It is important that the sending element be given first, followed by the receiving element (Table XIV).

Table XIV

Gain Plot Specifications

COLUMNS	FORMAT	DATA
1-5	I5	Total number of elements to be read
6-10	I5	Element number for sending element in 1st plot
11-15	I5	Element number for receiving element in 1st plot
16-20	I5	Element number for sending element in 2nd plot
21-25	I5	Element number for receiving element in 2nd plot

Standing Wave Plot Specifications

The last cards in the output section contain the remaining data for the Standing Wave Plots. The cards discussed here are only inserted if the standing wave options selected on Card 3 call for them (see Fig 21). No blank card should be inserted as was the case in the other output specifications (Ref 9: Sec 2, 52). Three cards are described, one for the Resonant Test Pressure plots and two for the Specific Pump Speed plots.

The first card in this group specifies the total number of components listed followed by the first and last system component used in each Resonant Test Pressure plot (Table XV). The program will then plot a standing wave plot at each pump speed where the peak pressure is greater than the resonant test pressure, for each set of components specified up to a maximum of 10 plots per component set.

The second and third card provide information for the Specific Pump Speed plots. The second card contains the component information, and is of the same format as the first card. In this case, the components specified are used for a single plot at the respective pump speed listed on the third card: the first two components are used with the first pump speed, the second two with the second speed and so on (Tables XV and XVI).

Table XV

First and Second Cards-Standing Wave Plots

COLUMNS	FORMAT	DATA	DIMENSIONS
1-5	I5	Total number of Components to be read	
6-10	I5	First Component in First plot	
11-15	I5	Last Component in First plot	
16-20	I5	First Component in Second Plot	
21-25	I5	Last Component in Second Plot	
26-30	I5	First Component in Third Plot	
31-35	I5	Last Component in Third Plot	
36-40	I5	First Component in Fourth Plot	
41-45	I5	Last Component in Fourth Plot	
46-50	I5	First Component in Fifth Plot	
51-55	I5	Last Component in Fifth Plot	
56-60	I5	First Component in Sixth Plot	
61-65	I5	Last Component in Sixth Plot	
66-70	I5	First Component in Seventh Plot	
71-75	I5	Last Component in Seventh Plot	

Table XVI

Third Card - Specific Pump Speeds

COLUMNS	FORMAT	DATA	DIMENSIONS
1-5	I5	Number of pump speeds on card	
6-15	F10.0	Pump speed for first plot	rpm
16-25	F10.0	Pump speed for second plot	rpm
26-35	F10.0	Pump speed for third plot	rpm
36-45	F10.0	Pump speed for fourth plot	rpm
46-55	F10.0	Pump speed for fifth plot	rpm
56-65	F10.0	Pump speed for sixth plot	rpm
66-75	F10.0	Pump speed for seventh plot-maximum number allowed	rpm

APPENDIX B

FLUID PROPERTY ESTIMATION

Appendix B

Fluid Property Estimation

The HSFR program determines values for three fluid properties: mass density ρ, kinematic viscosity ν, and bulk modulus β; based on the specified steady state temperature and pressure. Four fluids are described in the FLUID subroutine used in this investigation, replacing the three hydraulic oils described in the original HSFR program. The four fluids are Monomethyl Hydrazine (MMH), RP-1, Nitrogen Tetraoxide, (N_2O_4), and water. The main source of fluid property data for these fluids was Chapter 12 of the Aerospace Fluid Component Designers Handbook (Ref 22). The FLUID subroutine developed to describe these four fluids completely replaces the original subroutine, which contained data on three hydraulic oils (Ref 10: Sec 8, 3-7). A flow chart of the new subroutine is shown in Fig 23. Each section of this subroutine will be discussed in detail, beginning with the property data specification section.

Data Specification

The property data for density, kinematic viscosity and bulk modulus of the four fluids used in this investigation generally existed as temperature dependent, empirical equations or as temperature dependent tables. In a few cases, pressure was also included as a factor in determining the property. Tables XVII - XIX list this data in the units provided by the sources. Conversions to the units required by HSFR are accomplished by the subroutine. A check of the Design Handbook data (Ref 22) for the bulk modulus of MMH indicated that the temperature dependent equation and the value listed for 70°F differed by four orders of magnitude. Therefore, the FLUID subroutine computes the bulk modulus of MMH from the reported density and acoustic velocity relationships, using:
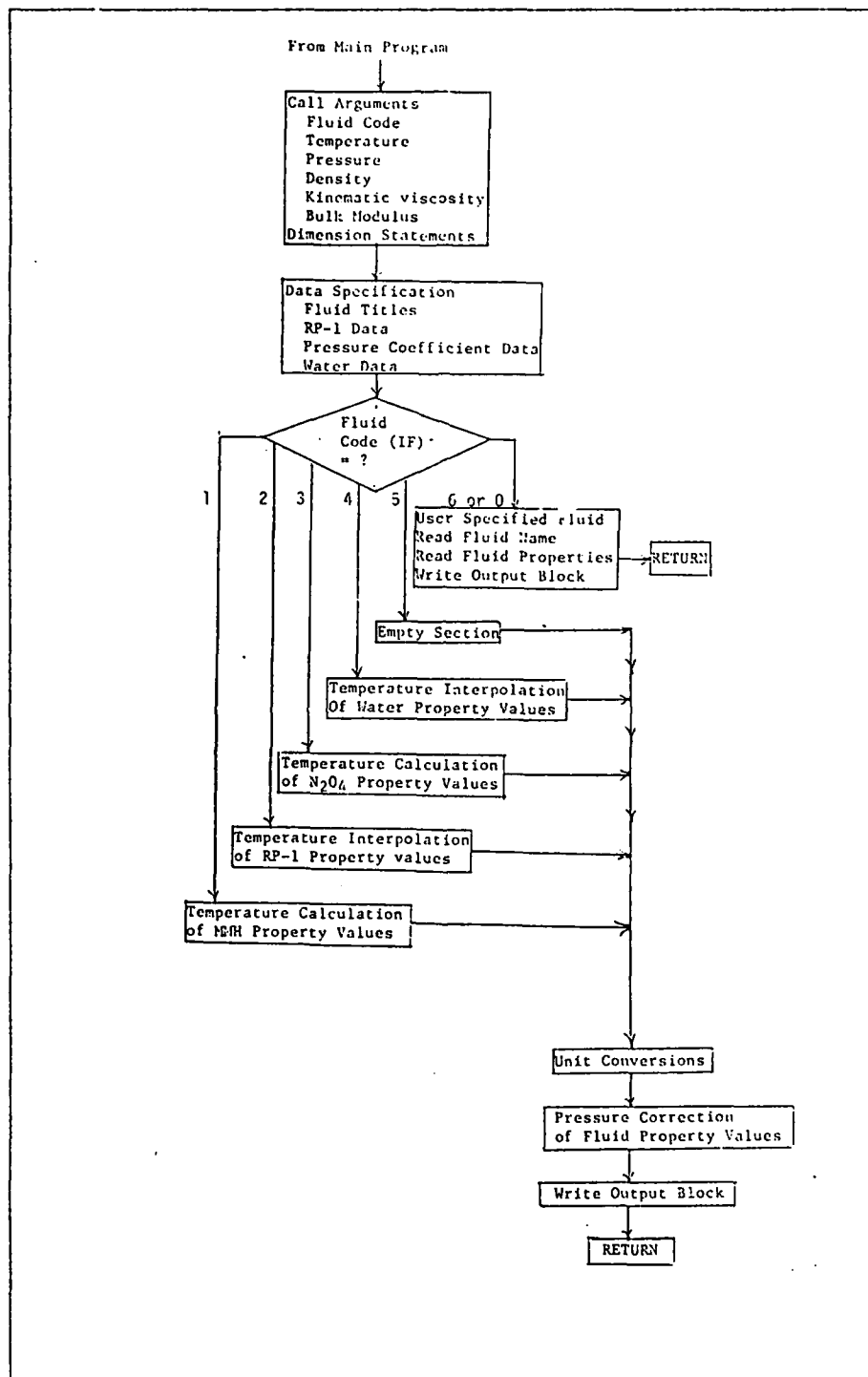
$$\beta = \frac{c^2 \rho}{g_c} \tag{7}$$

70

Fig 23. FLUID Subroutine Flow Chart

Table XVII

Fluid Property Data in Tabular Form

RP-1			
Temp (F)	Density (lbm/ft^3)	Kinematic Viscosity (cSt)	Bulk Modulus (psi)
-30.	51.25	16.40	179,000
0.	50.9	5.85	179,000
100.	49.3	1.65	179,000
300.	44.4	0.55	179,000

****

Water			
Temp (F)	Density (lbm/ft^3)	Kinematic Viscosity (ft^2/sec)	Bulk Modulus (psi)
32.	62.43	1.93×10^{-5}	285,000
60.	62.37	1.22×10^{-5}	313,000
100.	62.00	0.74×10^{-5}	331,000
150.	61.22	0.47×10^{-5}	328,000
212.	59.84	0.32×10^{-5}	300,000

Table XVIII

Temperature Dependent Equations for MMH

Density (lbm/ft^3) $\rho = 56.86 - (0.0321(T))$

Abs Visc (lbm/ft-sec) $\log \mu = -11.3266 + \dfrac{11284.}{R} - \dfrac{5796300.}{R^2} + \dfrac{1.10399 \times 10^9}{R^3}$

Kine Viscosity (in^2/sec) $\nu = \dfrac{\mu}{\rho} \times 144$

Acoustic Velocity (ft/sec) $c = 5629.5 - 7.113(T)$

Bulk Modulus (psi) $\beta = \dfrac{c^2 \rho}{4633.056}$

Table XIX

Temperature Dependent Equations for N_2O_4

$$\rho_s = 95.26 - 0.0657(T) - 1.1\times10^{-4}(T^2)$$
$$+2.19\times10^{-4}(P_s) + 4.94\times10^{-4}(P_s)(T)$$

Density (lbm/ft^3)

Abs Viscosity (lbm/ft-sec) $\mu = 1.347\times10^{-4} - \dfrac{8.710\times10^{-2}}{R} + \dfrac{161.8}{R^2}$

Kine Viscosity (in^2/sec) $\nu = \dfrac{\mu}{\rho} \times 144$

Bulk Modulus (psi)
$$\frac{1}{\beta} = 3.394\times10^{-6} + 1.26\times10^{-8}(T)$$
$$+1.486\times10^{-10}(T^2) - 6.329\times10^{-13}(T^3)$$

Values of the kinematic viscosity of the three propellants are computed from the density and absolute viscosity data reported in Ref 22. In the case of RP-1, where all data are in tabular form, the kinematic viscosity table was generated and used in the subroutine. Daugherty and Franzini (Ref 23) provided data on the kinematic viscosity of water for a series of temperatures.

The FLUID subroutine also requires a pressure coefficient σ for each fluid, which is used in correcting the kinematic viscosity for the effects of pressure (Table XX. According to a study done under contract to the Materials Laboratory, Air Force Wright Aeronautical Laboratories (Ref 24) the viscosity of hydraulic oils is related to the pressure by the expression:

$$\nu_s = \nu_0 \exp(\ \sigma^{TC}\ F_s\ 2.3\times10^{-4})\qquad(8)$$

This pressure coefficient σ is a function of the kinematic viscosity at atmospheric pressure and 100°F; and the ASTM slope determined from the ASTM Standard Viscosity-Temperature Chart E (Fig 24), which is no longer published by ASTM.

Table XX Pressure Coefficient Values

Fluid	ASTM	Slope
MMH	1.18	.013
RP-1	.808	.160
N_2O_4	*	.0001
H_2O	*	.0001
	*No ASTM Slope was determined	

The value of the pressure coefficient can be determined by the PRL Chart (Fig 25) or by the expression:

$$\sigma = D + E \log(\nu_0) + F(\log(\nu_0))^2 \qquad (9)$$

The values of the constants D, E, and F for a range of ASTM slopes are given in Table XXI (Ref 24:72). The factor of 2.3 is required in the exponent of Eq 8 to account for the PRL Chart being plotted on base 10 log scales as opposed to natural log scales (Ref 10:Appendix B,3). Since Eq 9 is derived from data plotted on the PRL Chart, the correction is required for pressure coefficients determined by Eq 9 also (Ref 24:73). Equation 9 was used instead of the PRL Chart for this investigation. The viscosity-pressure relation of Eq 8 decreases in accuracy when the kinematic viscosity approaches the lower limit of the ASTM chart used by this method, which is 2 cSt. By comparison, the kinematic viscosity of water is 0.68 cSt. Because the viscosities of water and N_2O_4 are below this 2 cSt limit, no ASTM slope could be determined for these fluids. The pressure coefficients for water and N_2O_4 were arbitrarily set at 0.0001, which forces the pressure correction factor of Eq 8 to approach 1, or a correction of zero.
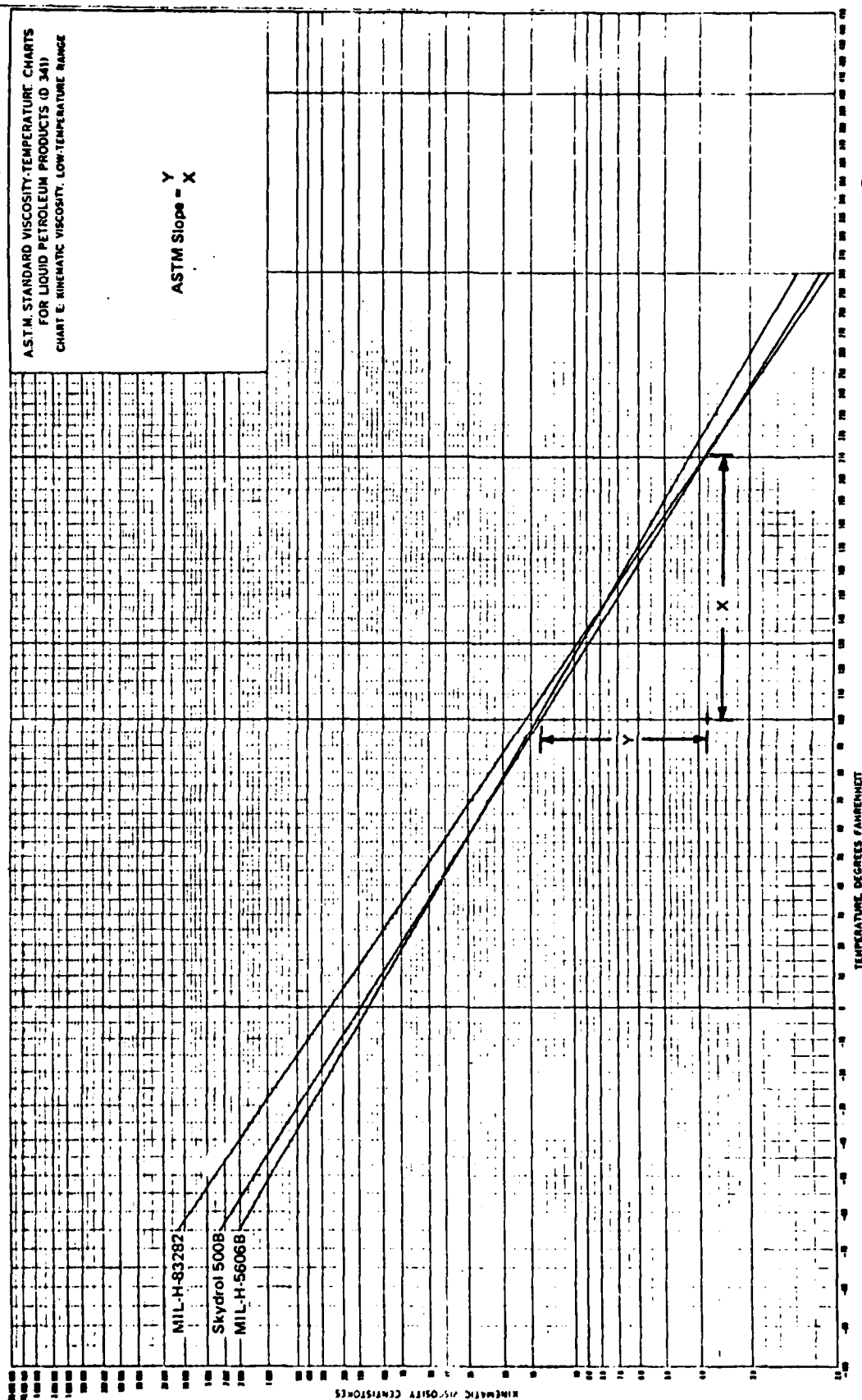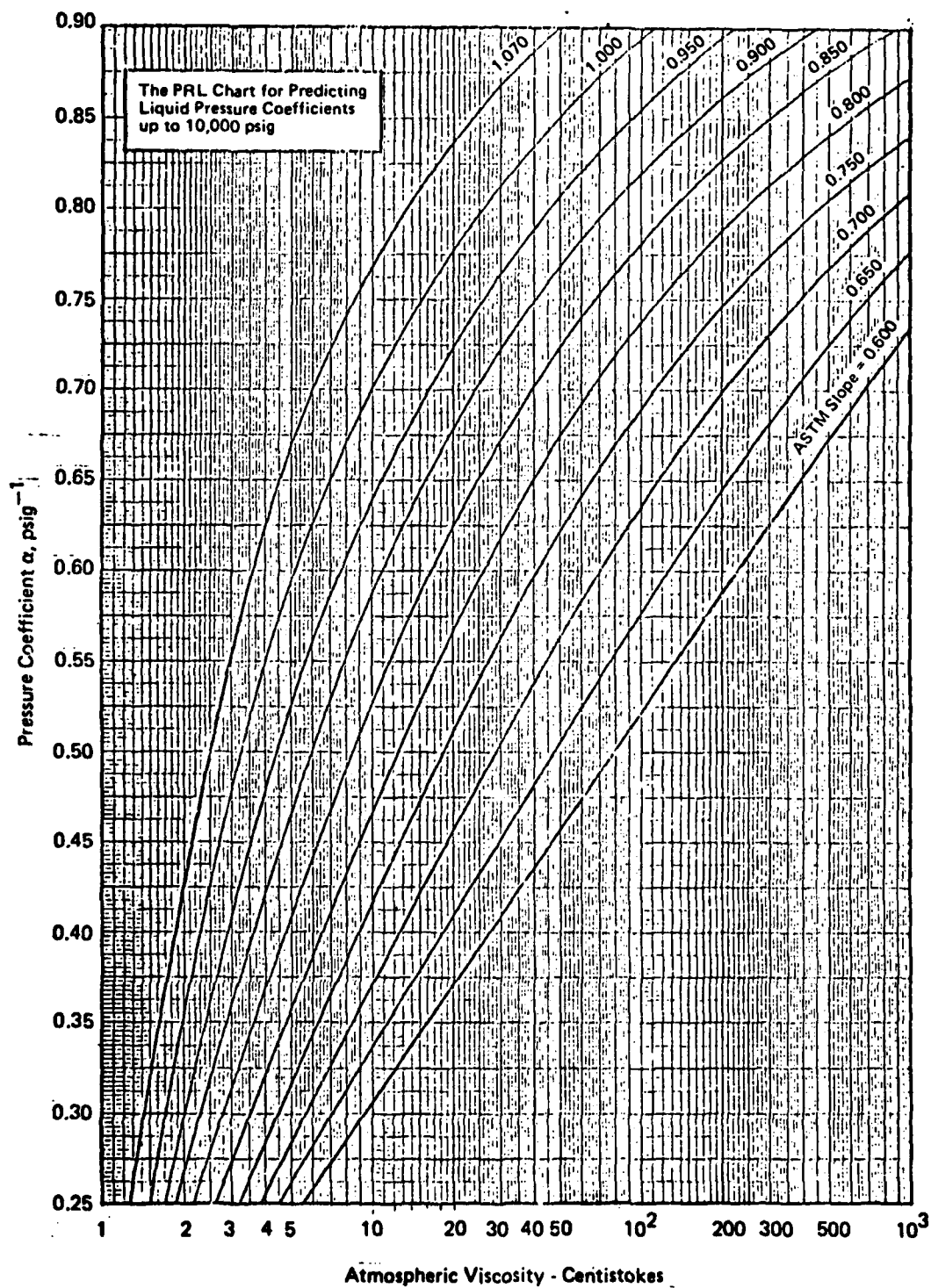
Fig 24. ASTM Viscosity Temperature Chart

75

Fig 25. PRL Chart for Pressure Coefficients

Table XXI

Coefficients Used in Pressure Coefficient Equation (Ref 24:72)

ASTM Slope	D	E	F
0.60	0.0878	0.2187	-0.0009
0.65	0.0578	0.2953	-0.0176
0.70	0.0425	0.3760	-0.0395
0.75	0.0379	0.4519	-0.0626
0.80	0.0546	0.5045	-0.0809
0.85	0.0720	0.5630	-0.1046
0.90	0.0947	0.6319	-0.1368
1.00	0.1384	0.8042	-0.2364
1.07	0.1423	1.0490	-0.4186

Steady State Temperature and Pressure Calculations

The FLUID subroutine uses the tabulated data or the empirical equations shown in Tables XVII through XIX to determine the property values at the steady state temperature. For the tabulated data for water and for the density data for RP-1, this temperature is interpolated by a second order Lagrange interpolation using the LAGRAN subroutine in HSFR. For the viscosity interpolation of RP-1, a modified Walther equation is used. This equation is the basis for the ASTM charts (Ref 10: Sec 8, 15):

$$\log\,(\log(v_0 + c))\, =\, A\,\log(R)\, +\, B \qquad (10)$$

Where

c = a constant, 0.6 in HSFR

A, B = Constants determined for the fluid

v_0 = Kinematic Viscosityt in cSt

This interpolation procedure is discussed in detail in the HSFR Technical Manual (Ref 10: Sec 8, 3-18). The property calculations for MMH and N_2O_4, which have

empirical equations, are done by solving the equations with the specified input conditions.

After calculating the three fluid properties at the steady state temperature, the three properties were converted from the units used in the temperature calculations to those used in the main program, as given in the nomenclature. Next, the properties were corrected for the effects of pressure. During this investigation, the pressure used in the HSFR analyses of the water filled experimental propellant system varied from 58 psia to 130 psia pump inlet pressure. The pump outlet pressure in the model ranged between 1000 and 3000 psia.

There is very little information about the effect of pressure on the properties of the four fluids of interest to this study. The Design Handbook (Ref 22) reports the density of N_2O_4 as a function of temperature and pressure. At -30^oF, a 100% increase in pressure yields a 0.001% increase in density, while at 300^oF, a 100% increase in pressure yields a 2% increase in density. The ASME Steam Tables (Ref 25) show that the kinematic viscosity of water decrease 8% as the pressure is increased from atmospheric to 12,000 psia. A review of data on the bulk modulus of water presented in The Handbook of Fluid Dynamics (Ref 26) showed that the pressure effect on bulk modulus can be represented by:

$$\beta_s = \beta_0 + (6.34 \ (P_s - 14.7)) \tag{11}$$

The use of this approximation instead of the tabulated data introduces a maximum of 1% error in the bulk modulus of water at 32^oF and 4500 psia, and 0.4% error for room temperature and 4500 psia. Due to the similarity towards water, this correction of 6.34 is applied to the bulk modulus correction of MMH and RP-1 also, as opposed to the correction factor of 12 used by HSFR for hydraulic oils.

The expression for correcting the density to the steady-state pressure is:

$$\rho_S = \rho_0 (1 + \frac{P_S}{262000}) \tag{12}$$

where the factor 262,000 is the average secant bulk modulus at 50°F and 100 psia for the four fluids in the subroutine. The correction of the kinematic viscosity for the effects of pressure has been discussed earlier, in the explanation of the pressure coefficient data. Unit conversions are done as required during the calculation of the fluid property values. The pressure correction equations are shown in Table XXII.

Table XXII

Pressure Correction Equations

Density	$\rho_S = \rho_0 (1 + \frac{P_S}{262000})$
Kinematic Viscosity	$\nu_S = \nu_0 \exp(\sigma^{TC} P_S \ 2.3 \times 10^{-4})$
Bulk Modulus	$\beta_S = \beta_0 + (6.34(P_S - 14.7)$

User Defined Fluid Properties

One feature of the original FLUID subroutine which was retained in the new subroutine is the option for the fluid properties to be specified as part of the input data. This option was very necessary during this investigation, as the propellant system inlet pressure was an order of magnitude lower than the pump outlet pressure, and the FLUID subroutine uses the pump outlet pressure in its calculations. Thus, for many of the computer runs during this investigation, the low pressure properties were directly input into the program. An additional advantage of the user defined fluid property option was in determining the sensitivities of the individual properties in the frequency response predictions.

APPENDIX C

EQUIVALENCY OF THOMSON AND KELVIN FUNCTIONS

Appendix C

Equivalency of Thomson and Kelvin Functions

D'Souza and Oldenberger's solution for the frequency dependent friction damping factor B, involves Thomson functions, ber and bei, of the zero and first order (Ref 4:592):

$$B = \frac{1}{\left[-\frac{2}{\alpha j^{\frac{1}{2}}} \frac{ber_1(\alpha) + j\ bei_1(\alpha)}{ber\ (\alpha) + j\ bei\ (\alpha)} + 1 \right]^{\frac{1}{2}}} \tag{13}$$

where
$$\alpha = r\left(\frac{\omega}{\nu}\right)^{\frac{1}{2}}$$

The Thomson functions were not referred to in any mathematical references consulted during this investigation, although Ref 16 discussed Kelvin functions and labeled them ber and bei, the same symbols as used for the Thomson functions. In D'Souza and Oldenburger's derivation:

$$ber_1(\alpha) + j\ bei_1(\alpha) = J_1(-\alpha j^{\frac{1}{2}})$$
$$ber\ (\alpha) + j\ bei\ (\alpha) = J_0(-\alpha j^{\frac{1}{2}}) \tag{14}$$

In Ref 16 the Kelvin functions are defined as

$$ber_1(\alpha) + j\ bei_1(\alpha) = J_1(\chi\ exp(j\ \tfrac{3\pi}{4}))$$
$$ber\ (\alpha) + j\ bei\ (\alpha) = J_0(\chi\ exp(j\ \tfrac{3\pi}{4})) \tag{15}$$

The two functions are equivalent if the right hand sides of Eqs 14 and 15 are equal, and the Bessel functions will be equal if the arguments are equal. Therefore, if the table of Kelvin function values in Ref 16 is valid for the solution of Eq 13, then

$$- j^{\frac{1}{2}} \overset{?}{=} exp(j\ \tfrac{3\pi}{4}) \tag{16}$$

By Euler's formula:

$$\exp(j\ \frac{3\pi}{4}) = \cos(\frac{3\pi}{4}) + j\ \sin(\frac{3\pi}{4}) \qquad (17)$$

According to Kreyszig (Ref 27) the formula for the square roots of a complex function, $z = 0 - j$, is:

$$\sqrt{z} = \sqrt{r}\ (\cos\frac{\theta}{2} + j\ \sin\frac{\theta}{2}) \qquad (18)$$

In polar form r is the modulus of z:

$$r = \sqrt{x^2 + y^2}$$

and θ is the argument of z:

$$\begin{aligned} \theta &= \sin^{-1}(\frac{y}{r}) \\ &= \sin^{-1}(\frac{-1}{1}) \\ &= \sin^{-1}(\frac{3}{2}) \end{aligned} \qquad (19)$$

Substituting for r and θ in Eq 18

$$(0 - j)^{\frac{1}{2}} = \cos\frac{3\pi}{4} + j\ \sin\frac{3\pi}{4} \qquad (20)$$

which is identical to Eq 17, thus

$$-j^{\frac{1}{2}} = \exp(j\ \frac{3\pi}{4})$$

and the Kelvin functions tabulated in Ref 16 are valid for solution of the frequency dependent friction damping factor B.

Vita

Bryan Scott DeHoff was born ██ ██████████████████████████. In 1974 he graduated from ██████████████████████████████████, and entered the West Virginia University College of Engineering. In 1975, he was awarded a three year scholarship through the Air Force ROTC program. Upon completion of his studies in 1978, he received the degree of Bachelor of Science in Mechanical Engineering and Mechanics and a commission in the USAF. Selected to enter AFIT in the fall of 1978, Lt DeHoff spent that summer as a Research Associate for the Mechanical Engineering Department of West Virginia University.

Permanent Address: ████████████████
████████████████████

REPORT DOCUMENTATION PAGE

1a. REPORT SECURITY CLASSIFICATION		1b. RESTRICTIVE MARKINGS
UNCLASSIFIED		NONE

2a. SECURITY CLASSIFICATION AUTHORITY	3. DISTRIBUTION/AVAILABILITY OF REPORT
	Approved for public release; distribution unlimited
2b. DECLASSIFICATION/DOWNGRADING SCHEDULE	

4. PERFORMING ORGANIZATION REPORT NUMBER(S)	5. MONITORING ORGANIZATION REPORT NUMBER(S)
AFIT/GA/AA/80M-1	

6a. NAME OF PERFORMING ORGANIZATION	6b. OFFICE SYMBOL (If applicable)	7a. NAME OF MONITORING ORGANIZATION
Air Force Institute of Technology	AFIT/EN	

6c. ADDRESS (City, State and ZIP Code)	7b. ADDRESS (City, State and ZIP Code)
Wright Patterson AFB OH 45433	

8a. NAME OF FUNDING/SPONSORING ORGANIZATION	8b. OFFICE SYMBOL (If applicable)	9. PROCUREMENT INSTRUMENT IDENTIFICATION NUMBER

8c. ADDRESS (City, State and ZIP Code)	10. SOURCE OF FUNDING NOS.			
	PROGRAM ELEMENT NO.	PROJECT NO.	TASK NO.	WORK UNIT NO.

11. TITLE (Include Security Classification)
See Reverse

12. PERSONAL AUTHOR(S)
Bryan S. DeHoff

13a. TYPE OF REPORT	13b. TIME COVERED		14. DATE OF REPORT (Yr., Mo., Day)	15. PAGE COUNT
MS Thesis	FROM _____ TO _____		84 December	93

16. SUPPLEMENTARY NOTATION

Approved for public release: IAW AFR 190-17.

LYNN E. WOLAVER 25 Feb 85
Dean for Research and Professional Development
Air Force Institute of Technology (ATC)
Wright-Patterson AFB OH 45433

17.	COSATI CODES		18. SUBJECT TERMS (Continue on reverse if necessary and identify by block number)
FIELD	GROUP	SUB. GR.	Liquid Rocket Feed Systems, Frequency Response, HSFR, Computer Program.
21	08	Thesis	

19. ABSTRACT (Continue on reverse if necessary and identify by block number)

This investigation applies the Hydraulic System Frequency Response (HSFR) computer program to a liquid propellant feed system analysis. During this investigation, the HSFR program was used to predict the oscillatory pressure, flow and impedance conditions existing in an experimental Saturn V first stage LOX suction duct. When necessary to model this system, additional capabilities were added to the program during this investigation. The results from the HSFR analysis are compared to previously published experimental and analytical data for this system. In this comparison, the HSFR program computed resonant frequencies which were between 0 and 3.6% higher than the test data. The sensitivity of the results to changes in the input model was also investigated. The results from this investigation indicate that the theoretical approach of the HSFR program is valid for large diameter feed systems, and recommendations for further model improvements are made.

20. DISTRIBUTION/AVAILABILITY OF ABSTRACT	21. ABSTRACT SECURITY CLASSIFICATION
UNCLASSIFIED/UNLIMITED ☒ SAME AS RPT. ☐ DTIC USERS ☐	UNCLASSIFIED

22a. NAME OF RESPONSIBLE INDIVIDUAL	22b. TELEPHONE NUMBER (Include Area Code)	22c. OFFICE SYMBOL
Dr Milton E. Franke	(513) 255-2362	AFIT/ENY

DD FORM 1473, 83 APR   EDITION OF 1 JAN 73 IS OBSOLETE.   UNCLASSIFIED

BLK 11 Title: APPLICATION OF THE HYDRAULIC SYSTEM FREQUENCY RESPONSE PROGRAM TO
PROPELLANT FEED SYSTEMS

END